Solving $\mathrm{SU}(3)$ Yang-Mills theory on the lattice: a calculation of selected gauge observables with gradient flow

Hans Mathias Mamen Vege
June 23, 2019

Supervisor: *Andrea Shindler*
Co-supervisor: *Morten Hjorth-Jensen*

University of Oslo

Introduction

Structure

- Quantum Chromodynamics(QCD).

- **QCD.** We will go through and explain what QCD as well as motivate its existence.

Structure

- Quantum Chromodynamics(QCD).
- Lattice QCD.

- **QCD.** We will go through and explain what QCD as well as motivate its existence.
- **LQCD.** We will briefly show how one discretise the lattice and perform calculations on it.

Structure

- Quantum Chromodynamics(QCD).
- Lattice QCD.
- Gradient flow.

- **QCD.** We will go through and explain what QCD as well as motivate its existence.
- **LQCD.** We will briefly show how one discretise the lattice and perform calculations on it.
- **Gradient flow.** We will quickly introduce gradient flow and explain its effects.

Structure

- Quantum Chromodynamics(QCD).
- Lattice QCD.
- Gradient flow.
- Developing a code for solving $\mathrm{SU}(3)$ Yang-Mills theory.

- **QCD.** We will go through and explain what QCD as well as motivate its existence.
- **LQCD.** We will briefly show how one discretise the lattice and perform calculations on it.
- **Gradient flow.** We will quickly introduce gradient flow and explain its effects.
- **GLAC.** Will briefly present the code which we developed as well as some benchmarks. We will also present the Metropolis algorithm.

Structure

- Quantum Chromodynamics(QCD).
- Lattice QCD.
- Gradient flow.
- Developing a code for solving $\mathrm{SU}(3)$ Yang-Mills theory.
- Results.

- **QCD.** We will go through and explain what QCD as well as motivate its existence.
- **LQCD.** We will briefly show how one discretise the lattice and perform calculations on it.
- **Gradient flow.** We will quickly introduce gradient flow and explain its effects.
- **GLAC.** Will briefly present the code which we developed as well as some benchmarks. We will also present the Metropolis algorithm.
- **Results.** We will present the results obtained from pure gauge calculations.

Structure

- Quantum Chromodynamics(QCD).
- Lattice QCD.
- Gradient flow.
- Developing a code for solving $\mathrm{SU}(3)$ Yang-Mills theory.
- Results.

Quantum Chromodynamics(QCD)

The Standard Model

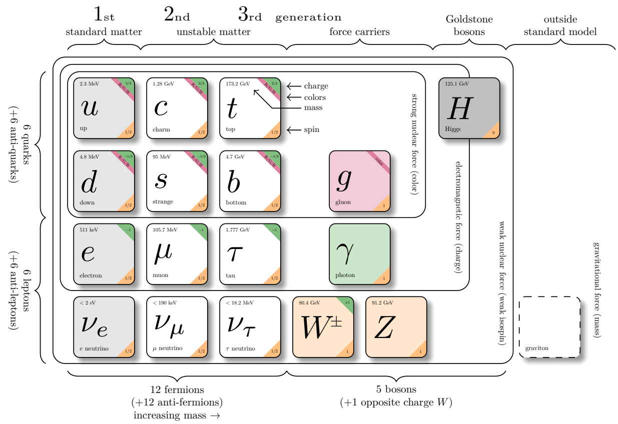

Consists of the innermost square of the **six quarks** and the *eight gluons*.

The QCD Lagrangian

$$\mathcal{L}_{\mathrm{QCD}} = \sum_{f=1}^{N_f} \bar{\psi}^{(f)} \left(i\not{D} - m^{(f)} \right) \psi^{(f)} - \frac{1}{4} G^a_{\mu\nu} G^{a\mu\nu},$$

with action

$$S = \int \mathrm{d}^4 x \mathcal{L}_{\mathrm{QCD}}, \tag{1}$$

is invariant under a $\mathrm{SU}(3)$ symmetry.

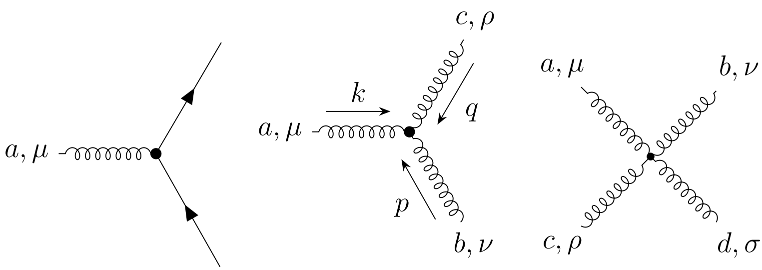

- *Gluon self-interaction.*
- This central aspect is mostly covered in the pure-gauge/Yang-Mills section of the theory.
- **Two important features**: *confinement* and *asymptotic freedom*.

Asymptotic freedom

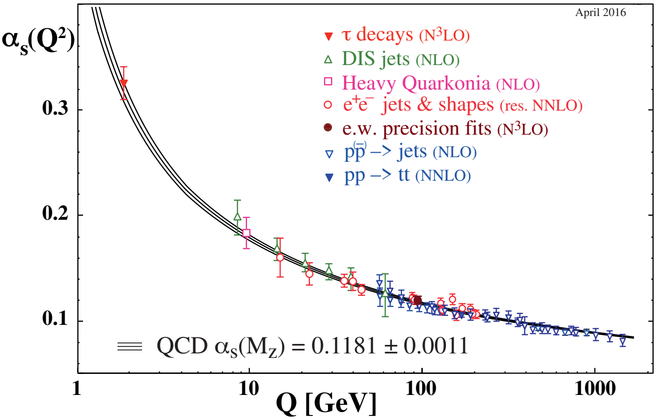

- The coupling constant **decreases** as we **increase** the energy.
- Also serves as an *experimental proof* of QCD.
- Other lines of *evidence*: triple γ decay and muon cross section ratio R.
  - Triple γ decay: the number of colors is included in the cross section, which can be measured experimentally.
  - Muon cross section ratio R: the ratio is dependent on having three colors.

Confinement

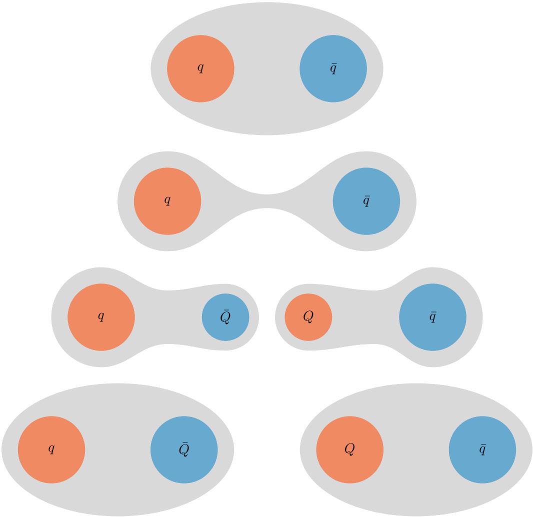

If we try to pull apart **two quarks in a meson**, more and more energy is required until we have enough energy to spontaneously create a **quark-antiquark** pair, forming thus **two new mesons.**

Lattice Quantum Chromodynamics(LQCD)

Discretizing spacetime

1. Divide spacetime into a cube of size $N^3 \times N_T$.

Make a quick drawing perhaps of a lattice?

Discretizing spacetime

1. Divide spacetime into a cube of size $N^3 \times N_T$.
2. Fermions live on the each *point* in the cube.

Make a quick drawing perhaps of a lattice?

Discretizing spacetime

1. Divide spacetime into a cube of size $N^3 \times N_T$.
2. Fermions live on the each *point* in the cube.
3. The gauge fields live on the sites *in between* the points, and is called links.

Make a quick drawing perhaps of a lattice?

Discretizing spacetime

1. Divide spacetime into a cube of size $N^3 \times N_T$.
2. Fermions live on the each *point* in the cube.
3. The gauge fields live on the sites *in between* the points, and is called links.

Goal: *maintain gauge invariance.*

Make a quick drawing perhaps of a lattice?

Links

A link connects one lattice site to another and is a $\mathrm{SU}(3)$ matrix.

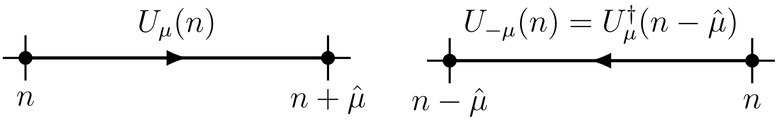

where $U_{-\mu}(n) = U_\mu(n-\hat{\mu})^\dagger$.

- Defined from the gauge transporter.
- A link in the positive $\hat{\mu}$ direction is shown in the figure to the left.
- A link in the negative $\hat{\mu}$ direction is shown in the figure to the right.

Gauge invariance on the lattice

Links constructed such that we maintain gauge invariance in the action,

Links constructed such that we maintain gauge invariance in the action,

$$U_\mu(n) \to U'_\mu(n) = \Omega(n)\, U_\mu(n)\Omega(n+\hat{\mu})^\dagger,$$
$$U_{-\mu}(n) \to U'_{-\mu}(n) = \Omega(n)\, U_\mu(n-\hat{\mu})^\dagger\Omega(n-\hat{\mu})^\dagger.$$

Gauge invariance on the lattice

Links constructed such that we maintain gauge invariance in the action,

$$
\begin{aligned}
U_\mu(n) &\to U'_\mu(n) = \Omega(n)\, U_\mu(n)\Omega(n+\hat{\mu})^\dagger, \\
U_{-\mu}(n) &\to U'_{-\mu}(n) = \Omega(n)\, U_\mu(n-\hat{\mu})^\dagger\Omega(n-\hat{\mu})^\dagger.
\end{aligned}
$$

Two main types of gauge invariant objects,

Gauge invariance on the lattice

Links constructed such that we maintain gauge invariance in the action,

$$
\begin{aligned}
U_\mu(n) &\to U'_\mu(n) = \Omega(n)\, U_\mu(n)\Omega(n+\hat{\mu})^\dagger, \\
U_{-\mu}(n) &\to U'_{-\mu}(n) = \Omega(n)\, U_\mu(n-\hat{\mu})^\dagger\Omega(n-\hat{\mu})^\dagger.
\end{aligned}
$$

Two main types of gauge invariant objects,

- Objects with fermions ψ, $\bar{\psi}$ as end points.

Links constructed such that we maintain gauge invariance in the action,

$$U_\mu(n) \to U'_\mu(n) = \Omega(n)\, U_\mu(n)\Omega(n+\hat{\mu})^\dagger,$$
$$U_{-\mu}(n) \to U'_{-\mu}(n) = \Omega(n)\, U_\mu(n-\hat{\mu})^\dagger\Omega(n-\hat{\mu})^\dagger.$$

Two main types of gauge invariant objects,

- Objects with fermions ψ, $\bar{\psi}$ as end points.
- Fully connected gauge invariant objects(i.e. “loops”).

The plaquette

The simplest gauge invariant object,

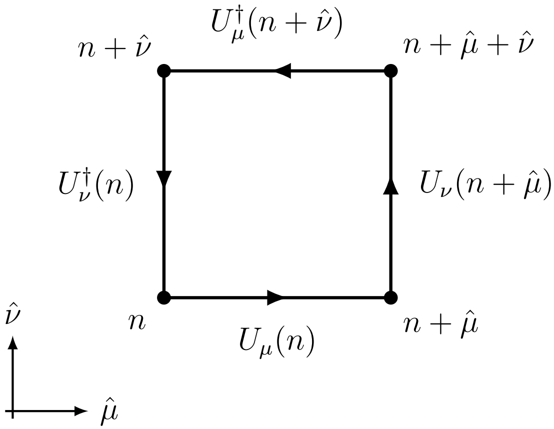

The Wilson gauge action

The Wilson gauge action is given as

$$S_G[U] = \frac{\beta}{3} \sum_{n \in \Lambda} \sum_{\mu < \nu} \mathrm{Re}\,\mathrm{tr}\left[1 - P_{\mu\nu}(n)\right],$$

with $\beta = 6/g_S^2$.

Continuum gauge action,

$$S_G[A] = \frac{1}{2g_S^2} \int \mathrm{d}^4x \mathrm{tr} F_{\mu\nu}^2,$$

recovered when $a \to 0$.

- Using the definition of the link we saw earlier, we can reproduce the continuum action up to an discretization error of $\mathcal{O}(a^2)$.

Developing a code for solving $\mathrm{SU}(3)$ Yang-Mills theory on the lattice

The numerical challenge in lattice QCD

A lattice configuration consists of 3×3 $\mathrm{SU}(3)$ matrices,

- The $\mathrm{SU}(3)$ matrices are 3×3 matrices of nine complex numbers or 18 real numbers.
- This leads to an absolute **requirement of efficiency**, both in **calculations** and in **input/output**.
- When returning to what ensembles of configurations we generated this will be evident.

The numerical challenge in lattice QCD

A lattice configuration consists of 3×3 $\mathrm{SU}(3)$ matrices,

$$\underbrace{N^3}_{\text{Spatial}} \times \underbrace{N_T}_{\text{Temporal}} \times \underbrace{4}_{\text{Links}} \times \underbrace{9}_{\mathrm{SU}(3)\text{ matrix}} \times \underbrace{2}_{\mathbb{C}\text{-numbers}} = 72 N^3 N_T,$$

- The $\mathrm{SU}(3)$ matrices are 3×3 matrices of nine complex numbers or 18 real numbers.
- This leads to an absolute **requirement of efficiency**, both in **calculations** and in **input/output**.
- When returning to what ensembles of configurations we generated this will be evident.

The numerical challenge in lattice QCD

A lattice configuration consists of 3×3 $\mathrm{SU}(3)$ matrices,

$$\underbrace{N^3}_{\text{Spatial}} \times \underbrace{N_T}_{\text{Temporal}} \times \underbrace{4}_{\text{Links}} \times \underbrace{9}_{\mathrm{SU}(3)\text{ matrix}} \times \underbrace{2}_{\mathbb{C}\text{-numbers}} = 72N^3N_T,$$

$\rightarrow 8 \times 72N^3N_T$ bytes.

- The $\mathrm{SU}(3)$ matrices are 3×3 matrices of nine complex numbers or 18 real numbers.
- This leads to an absolute **requirement of efficiency**, both in **calculations** and in **input/output**.
- When returning to what ensembles of configurations we generated this will be evident.

The path integral

$$\langle O \rangle = \frac{1}{Z} \int \mathcal{D}U \mathcal{D}\psi \mathcal{D}\bar{\psi}\, O[\psi, \bar{\psi}, U] \mathrm{e}^{-S_G[U] - S_F[\psi, \bar{\psi}, U]}.$$

$$Z = \int \mathcal{D}U \mathcal{D}\psi \mathcal{D}\bar{\psi}\, e^{-S_G[U] - S_F[\psi, \bar{\psi}, U]}.$$

The path integral

$$\langle O \rangle = \frac{1}{Z} \int \mathcal{D}U O[U] \mathrm{e}^{-S_G[U]}.$$

$$Z = \int \mathcal{D}U e^{-S_G[U]}.$$

The path integral

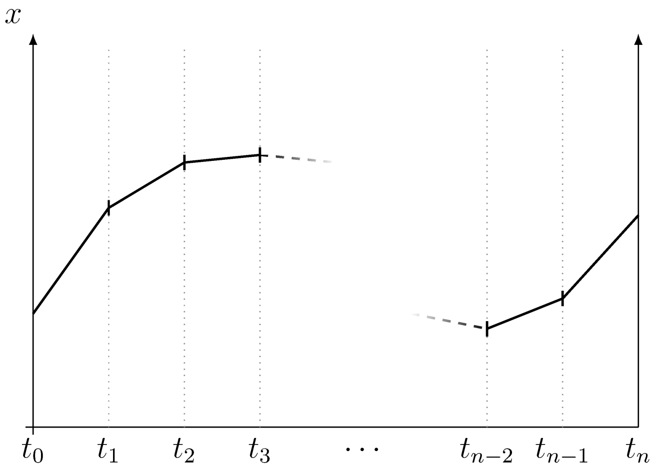

- An example of the discretized path integral, going from time t_0 to t_n, where the end points is taken to be equal, $x_0 = x_{N_T}$. We integrate over all of space at each time t_i finding the most likely position at a given time.

The path integral

$$\langle O \rangle = \frac{1}{Z} \int \mathcal{D}U \, O[U] \mathrm{e}^{-S_G[U]}.$$

with

$$Z = \int \mathcal{D}U e^{-S_G[U]}.$$

- An example of the discretized path integral, going from time t_0 to t_n, where the end points is taken to be equal, $x_0 = x_{N_T}$. We integrate over all of space at each time t_i finding the most likely position at a given time.
- We will use the parts marked in red as a probability distribution which we will create configurations from.

$$\langle O \rangle = \frac{1}{Z} \int \mathcal{D}U \, O[U] \mathrm{e}^{-S_G[U]}.$$

with

$$Z = \int \mathcal{D}U e^{-S_G[U]}.$$

We will use the *Metropolis algorithm* to create configurations of the lattice.

- An example of the discretized path integral, going from time t_0 to t_n, where the end points is taken to be equal, $x_0 = x_{N_T}$. We integrate over all of space at each time t_i finding the most likely position at a given time.
- We will use the parts marked in red as a probability distribution which we will create configurations from.
- This can be used in the *Metropolis algorithm*.

$$\langle O \rangle = \frac{1}{Z} \int \mathcal{D}U \, O[U] \mathrm{e}^{-S_G[U]}.$$

with

$$Z = \int \mathcal{D}U e^{-S_G[U]}.$$

We will use the *Metropolis algorithm* to create configurations of the lattice.

- An example of the discretized path integral, going from time t_0 to t_n, where the end points is taken to be equal, $x_0 = x_{N_T}$. We integrate over all of space at each time t_i finding the most likely position at a given time.
- We will use the parts marked in red as a probability distribution which we will create configurations from.
- This can be used in the *Metropolis algorithm*.
- Since a path integral integrates over all possible configurations, our job us to generate enough configurations to properly represent the statistics.

The path integral

$$\langle O \rangle = \frac{1}{Z} \int \mathcal{D}U \, O[U] \mathrm{e}^{-S_G[U]}.$$

with

$$Z = \int \mathcal{D}U e^{-S_G[U]}.$$

We will use the *Metropolis algorithm* to create configurations of the lattice.

- An example of the discretized path integral, going from time t_0 to t_n, where the end points is taken to be equal, $x_0 = x_{N_T}$. We integrate over all of space at each time t_i finding the most likely position at a given time.
- We will use the parts marked in red as a probability distribution which we will create configurations from.
- This can be used in the *Metropolis algorithm*.
- Since a path integral integrates over all possible configurations, our job us to generate enough configurations to properly represent the statistics.

The observable becomes an average over the N_{MC} gauge configurations.

$$\langle O \rangle = \lim_{N_{\mathrm{MC}} \to \infty} \frac{1}{N_{\mathrm{MC}}} \sum_{i}^{N_{\mathrm{MC}}} O[U_i]$$

We now need to generate configurations...

- We perform an average of the created configurations.

Parallelization

The lattice now is a 4D hypercube, with four links associated to each lattice site $\rightarrow$need to parallelize!

- Due to the size of the lattice, we need to parallelize!.

Parallelization

The lattice now is a 4D hypercube, with four links associated to each lattice site $\rightarrow$need to parallelize!

Two methods used:

- Due to the size of the lattice, we need to parallelize!.
- We parallelized using MPI.

The lattice now is a 4D hypercube, with four links associated to each lattice site →need to parallelize!

Two methods used:

- Single link sharing used in the Metropolis algorithm.

- Due to the size of the lattice, we need to parallelize!.
- We parallelized using **MPI**.
- Tested out **halos**, but turned out to be problematic when generating.

Parallelization

The lattice now is a 4D hypercube, with four links associated to each lattice site $\rightarrow$need to parallelize!

Two methods used:

- Single link sharing used in the Metropolis algorithm.
- *shifts* used in in gradient flow and observable sampling

- Due to the size of the lattice, we need to parallelize!.
- We parallelized using **MPI**.
- Tested out **halos**, but turned out to be problematic when generating.

Shifts

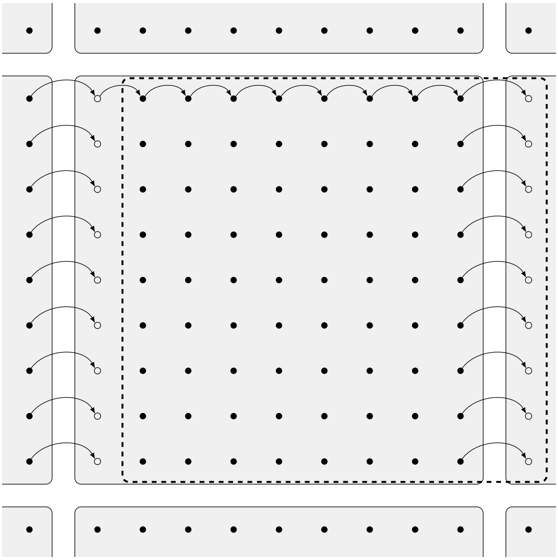

- An illustration of the lattice shift.
- The links U_ν of the lattice are copied over to a temporary lattice shifted in direction $\hat{\mu}$.
- The face that is shifted over to an adjacent sub-lattice is shared through a non-blocking MPI call, while we copy the links to the temporary lattice.
- Allows for a simplified syntax close to that of the equations we are working with.
- Don't have to write out any loops over the lattice positions.

Gradient flow

The flow equation

The flow of the $\mathrm{SU}(3)$ gauge fields are denoted by $B_\mu(x, t_f)$ which are Lie algebra valued gauge fields,

$$\frac{\mathrm{d}}{\mathrm{d}t_f} B_\mu(x, t_f) = D_\nu \, G_{\nu\,\mu}(x, t_f),$$

- The flow equation in the continuum is defined by this differential equation.

The flow equation

The flow of the $\mathrm{SU}(3)$ gauge fields are denoted by $B_\mu(x, t_f)$ which are Lie algebra valued gauge fields,

$$\frac{\mathrm{d}}{\mathrm{d}t_f} B_\mu(x, t_f) = D_\nu \, G_{\nu\,\mu}(x, t_f),$$

$$D_\mu = \partial_\mu + [B_\mu(x, t_f), \cdot] \,,$$

- The flow equation in the continuum is defined by this differential equation.
- With the covariant derivative given by following, with the · being the derivative with respect to flow time.

The flow equation

The flow of the $\mathrm{SU}(3)$ gauge fields are denoted by $B_\mu(x, t_f)$ which are Lie algebra valued gauge fields,

$$\frac{\mathrm{d}}{\mathrm{d}t_f} B_\mu(x, t_f) = D_\nu \, G_{\nu\,\mu}(x, t_f),$$

$$D_\mu = \partial_\mu + \left[B_\mu(x, t_f), \cdot\right],$$

$$G_{\mu\nu}(x, t_f) = \partial_\mu B_\nu(x, t_f) - \partial_\nu B_\mu(x, t_f) - i[B_\mu(x, t_f), B_\nu(x, t_f)],$$

- The flow equation in the continuum is defined by this differential equation.
- With the covariant derivative given by following, with the $\cdot$ being the derivative with respect to flow time.
- The field strength tensor of the flown fields is given in the regular format.

The flow equation

The flow of the $\mathrm{SU}(3)$ gauge fields are denoted by $B_\mu(x,t_f)$ which are Lie algebra valued gauge fields,

$$\frac{\mathrm{d}}{\mathrm{d}t_f} B_\mu(x,t_f) = D_\nu \, G_{\nu\,\mu}(x,t_f),$$

$$D_\mu = \partial_\mu + \left[B_\mu(x,t_f), \cdot\right],$$

$$G_{\mu\nu}(x,t_f) = \partial_\mu B_\nu(x,t_f) - \partial_\nu B_\mu(x,t_f) - i[B_\mu(x,t_f), B_\nu(x,t_f)],$$

with the initial conditions being the fundamental gauge field,

$$B_\mu(x,t_f)|_{t_f=0} = A_\mu(x).$$

- The flow equation in the continuum is defined by this differential equation.
- With the covariant derivative given by following, with the $\cdot$ being the derivative with respect to flow time.
- The field strength tensor of the flown fields is given in the regular format.
- The initial condition is the un-flowed gauge field, A_μ.

The flow equation

The flow of the $\mathrm{SU}(3)$ gauge fields are denoted by $B_\mu(x,t_f)$ which are Lie algebra valued gauge fields,

$$\frac{\mathrm{d}}{\mathrm{d}t_f} B_\mu(x,t_f) = D_\nu G_{\nu\,\mu}(x,t_f),$$

$$D_\mu = \partial_\mu + \left[B_\mu(x,t_f),\cdot\right],$$

$$G_{\mu\nu}(x,t_f) = \partial_\mu B_\nu(x,t_f) - \partial_\nu B_\mu(x,t_f) - i[B_\mu(x,t_f), B_\nu(x,t_f)],$$

with the initial conditions being the fundamental gauge field,

$$B_\mu(x,t_f)|_{t_f=0} = A_\mu(x).$$

A bad approximation: *the diffusion equation*,

$$\frac{\partial}{\partial t_f} B_\mu(x,t_f) \approx \partial^2 B_\mu(x,t_f)$$

- The flow equation in the continuum is defined by this differential equation.
- With the covariant derivative given by following, with the $\cdot$ being the derivative with respect to flow time.
- The field strength tensor of the flown fields is given in the regular format.
- The initial condition is the un-flowed gauge field, A_μ.
- Bad approx.: diffusion equation.

The flow equation

The flow of the $\mathrm{SU}(3)$ gauge fields are denoted by $B_\mu(x,t_f)$ which are Lie algebra valued gauge fields,

$$\frac{\mathrm{d}}{\mathrm{d}t_f} B_\mu(x,t_f) = D_\nu\, G_{\nu\,\mu}(x,t_f),$$

$$D_\mu = \partial_\mu + \left[B_\mu(x,t_f), \cdot\right],$$

$$G_{\mu\nu}(x,t_f) = \partial_\mu B_\nu(x,t_f) - \partial_\nu B_\mu(x,t_f) - i[B_\mu(x,t_f), B_\nu(x,t_f)],$$

with the initial conditions being the fundamental gauge field,

$$B_\mu(x,t_f)|_{t_f=0} = A_\mu(x).$$

A bad approximation: *the diffusion equation*,

$$\frac{\partial}{\partial t_f} B_\mu(x,t_f) \approx \partial^2 B_\mu(x,t_f)$$

The smearing radius increases as $\sqrt{8t_f}$.

- The flow equation in the continuum is defined by this differential equation.
- With the covariant derivative given by following, with the $\cdot$ being the derivative with respect to flow time.
- The field strength tensor of the flown fields is given in the regular format.
- The initial condition is the un-flowed gauge field, A_μ.
- Bad approx.: diffusion equation.
- Topological charge preserved and is more pronounced.
- Renormalizes the topological charge at non-zero flow time.

The flow equation

The flow of the $\mathrm{SU}(3)$ gauge fields are denoted by $B_\mu(x, t_f)$ which are Lie algebra valued gauge fields,

$$\frac{\mathrm{d}}{\mathrm{d}t_f} B_\mu(x, t_f) = D_\nu G_{\nu\,\mu}(x, t_f),$$

$$D_\mu = \partial_\mu + \left[B_\mu(x, t_f), \cdot\right],$$

$$G_{\mu\nu}(x, t_f) = \partial_\mu B_\nu(x, t_f) - \partial_\nu B_\mu(x, t_f) - i[B_\mu(x, t_f), B_\nu(x, t_f)],$$

with the initial conditions being the fundamental gauge field,

$$B_\mu(x, t_f)|_{t_f=0} = A_\mu(x).$$

A bad approximation: *the diffusion equation*,

$$\frac{\partial}{\partial t_f} B_\mu(x, t_f) \approx \partial^2 B_\mu(x, t_f)$$

The smearing radius increases as $\sqrt{8t_f}$.

- The flow equation in the continuum is defined by this differential equation.
- With the covariant derivative given by following, with the · being the derivative with respect to flow time.
- The field strength tensor of the flown fields is given in the regular format.
- The initial condition is the un-flowed gauge field, A_μ.
- Bad approx.: diffusion equation.
- Topological charge preserved and is more pronounced.
- Renormalizes the topological charge at non-zero flow time.

Gradient flow on the lattice

Lattice definition given by

$$\dot{V}_{t_f}(x,\mu) = -g_S^2 \left\{\partial_{x,\mu} S_G[V_{t_f}]\right\} V_{t_f}(x,\mu),$$

- On the lattice, the flow equation takes the shape in terms of the link variables.

Gradient flow on the lattice

Lattice definition given by

$$\dot{V}_{t_f}(x,\mu) = -g_S^2 \left\{\partial_{x,\mu} S_G[V_{t_f}]\right\} V_{t_f}(x,\mu),$$

with initial condition,

$$V_{t_f}(x,\mu)|_{t_f=0} = U(x,\mu)$$

- On the lattice, the flow equation takes the shape in terms of the link variables.
- Initial conditions similar to the continuum case.

Gradient flow on the lattice

Lattice definition given by

$$\dot{V}_{t_f}(x,\mu) = -g_S^2 \left\{\partial_{x,\mu} S_G[V_{t_f}]\right\} V_{t_f}(x,\mu),$$

with initial condition,

$$V_{t_f}(x,\mu)|_{t_f=0} = U(x,\mu)$$

Note: need to find the action derivative $S_G[V_{t_f}]$.

- On the lattice, the flow equation takes the shape in terms of the link variables.
- Initial conditions similar to the continuum case.
- The action derivative is also needed, but that is a minor task we will not cover here.

Gradient flow on the lattice

Lattice definition given by

$$\dot{V}_{t_f}(x,\mu) = -g_S^2 \left\{\partial_{x,\mu} S_G[V_{t_f}]\right\} V_{t_f}(x,\mu),$$

with initial condition,

$$V_{t_f}(x,\mu)|_{t_f=0} = U(x,\mu)$$

Note: need to find the action derivative $S_G[V_{t_f}]$.

- On the lattice, the flow equation takes the shape in terms of the link variables.
- Initial conditions similar to the continuum case.
- The action derivative is also needed, but that is a minor task we will not cover here.

Solving gradient flow with Runge-Kutta 3

With

$$\dot{V}_{t_f} = -g_S^2 \left\{ \partial_{x,\mu} S_G[V_{t_f}] \right\} V_{t_f} = Z(V_{t_f}) V_{t_f},$$

- We rewrite the equations slightly,

Solving gradient flow with Runge-Kutta 3

With

$$\dot{V}_{t_f} = -g_S^2 \left\{\partial_{x,\mu} S_G[V_{t_f}]\right\} V_{t_f} = Z(V_{t_f}) V_{t_f},$$

and $Z_i = \epsilon_f Z(W_i)$ we get

$$\begin{aligned}
W_0 &= V_{t_f}, \\
W_1 &= \exp\left[\frac{1}{4} Z_0\right] W_0, \\
W_2 &= \exp\left[\frac{8}{9} Z_1 - \frac{17}{36} Z_0\right] W_1, \\
V_{t_f+\epsilon_f} &= \exp\left[\frac{3}{4} Z_2 - \frac{8}{9} Z_1 + \frac{17}{36} Z_0\right] W_2,
\end{aligned}$$

with coefficients from Lüscher [3].

- We rewrite the equations slightly,
- and use a structure preserving integrator with coefficients from Lüscher [3].

Solving gradient flow with Runge-Kutta 3

With

$$\dot{V}_{t_f} = -g_S^2 \left\{\partial_{x,\mu} S_G[V_{t_f}]\right\} V_{t_f} = Z(V_{t_f}) V_{t_f},$$

and $Z_i = \epsilon_f Z(W_i)$ we get

$$\begin{aligned}
W_0 &= V_{t_f}, \\
W_1 &= \exp\left[\frac{1}{4} Z_0\right] W_0, \\
W_2 &= \exp\left[\frac{8}{9} Z_1 - \frac{17}{36} Z_0\right] W_1, \\
V_{t_f+\epsilon_f} &= \exp\left[\frac{3}{4} Z_2 - \frac{8}{9} Z_1 + \frac{17}{36} Z_0\right] W_2,
\end{aligned}$$

with coefficients from Lüscher [3].

- We rewrite the equations slightly,
- and use a structure preserving integrator with coefficients from Lüscher [3].
- We control the accuracy of this integrator by ϵ_f.

Solving gradient flow with Runge-Kutta 3

With

$$\dot{V}_{t_f} = -g_S^2 \left\{\partial_{x,\mu} S_G[V_{t_f}]\right\} V_{t_f} = Z(V_{t_f}) V_{t_f},$$

and $Z_i = \epsilon_f Z(W_i)$ we get

$$\begin{aligned}
W_0 &= V_{t_f}, \\
W_1 &= \exp\left[\frac{1}{4} Z_0\right] W_0, \\
W_2 &= \exp\left[\frac{8}{9} Z_1 - \frac{17}{36} Z_0\right] W_1, \\
V_{t_f+\epsilon_f} &= \exp\left[\frac{3}{4} Z_2 - \frac{8}{9} Z_1 + \frac{17}{36} Z_0\right] W_2,
\end{aligned}$$

with coefficients from Lüscher [3].

- We rewrite the equations slightly,
- and use a structure preserving integrator with coefficients from Lüscher [3].
- We control the accuracy of this integrator by ϵ_f.

- The Runge-Kutta 3 integrator has been tested for different step lengths ϵ_f.

Verifications, tests and code benchmarking

- The Runge-Kutta 3 integrator has been tested for different step lengths ϵ_f.
- The code has been unit tested for matrix multiplications and parallelization.

Verifications, tests and code benchmarking

- The Runge-Kutta 3 integrator has been tested for different step lengths ϵ_f.
- The code has been unit tested for matrix multiplications and parallelization.
- Results match that of other code bases such as Chroma.

- The Runge-Kutta 3 integrator has been tested for different step lengths ϵ_f.
- The code has been unit tested for matrix multiplications and parallelization.
- Results match that of other code bases such as Chroma.
- Performance testing has been done of different generation parameters.

Results

Ensemble	β	N	N_T	N_{cfg}	ϵ_{flow}	Config. size[GB]
A	6.0	24	48	1000	0.01	0.356
B	6.1	28	56	1000	0.01	0.659
C	6.2	32	64	2000	0.01	1.125
D_1	6.45	32	32	1000	0.02	0.563
D_2	6.45	48	96	250	0.02	5.695

- The main ensembles made for this thesis.
- Every configuration was flown with $N_{\text{flow}} = 1000$ flow steps.
- We should also mention that we generated a few additional ensembles for investigating other aspects of the topological charge.

Lattice sizes

Ensemble	L/a	L [fm]	a [fm]
A	24	2.235(9)	0.0931(4)
B	28	2.214(10)	0.0791(3)
C	32	2.17(1)	0.0679(3)
D_1	32	1.530(9)	0.0478(3)
D_2	48	2.29(1)	0.0478(3)

Charge radius of a proton: ~ 0.85 fm.

The lattice sizes.

Energy definition

$$E = \frac{a^4}{2|\Lambda|} \sum_{n \in \Lambda} \sum_{\mu,\nu} \left(F^{\text{clov}}_{\mu\nu}(n) \right)^2$$

- Defined as the field strength tensor squared averaged over all lattice points and directions.
- We can use this definition to set a scale.

Energy definition

$$E = \frac{a^4}{2|\Lambda|} \sum_{n\in\Lambda} \sum_{\mu,\nu} \left(F^{\mathrm{clov}}_{\mu\nu}(n)\right)^2$$

We can use this definition to set a scale t_0,

$$\left\{t_f^2 \langle E(t)\rangle\right\}_{t_f=t_0} = 0.3.$$

- Defined as the field strength tensor squared averaged over all lattice points and directions.
- We can use this definition to set a scale.

The clover field strength definition

$F^{\text{clov}}_{\mu\nu}(n)$ is given by

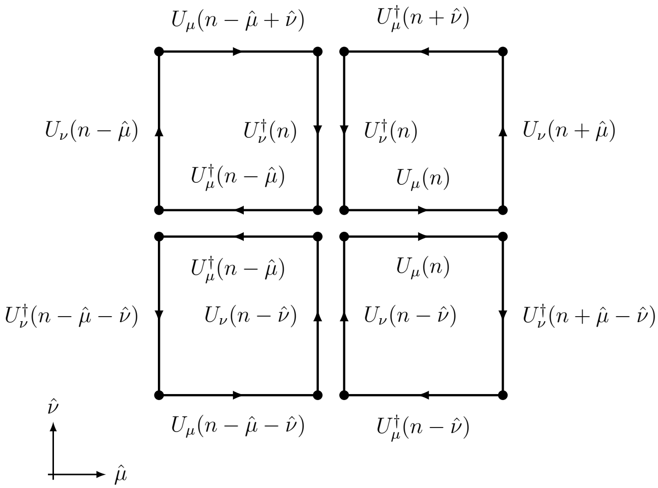

- We will use the clover field strength definition in gauge observables.
- **Symmetries** will allow us to **reduce** the effective **number of clovers** need to **calculate from 24 to 6**.

Energy

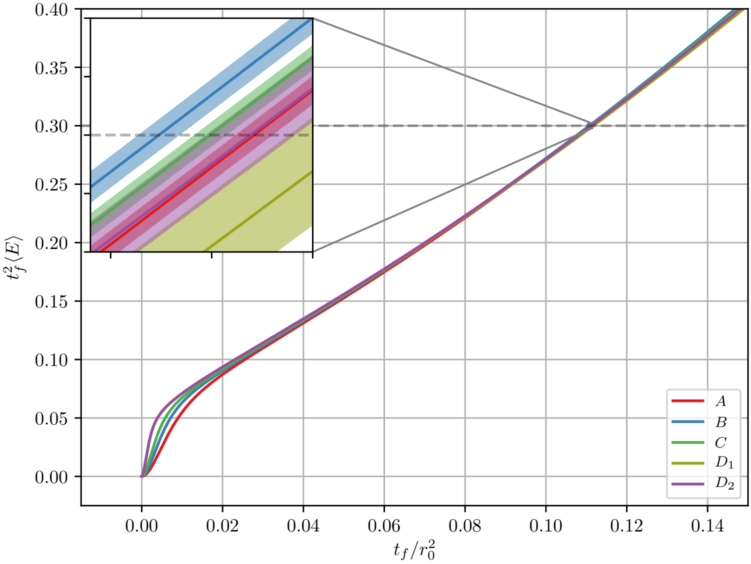

0.40
0.35
0.30
0.25
0.20
0.15
0.10
0.05
0.00
$t_f^2\langle E\rangle$
0.00
0.02
0.04
0.06
0.08
0.10
0.12
0.14
t_f/r_0^2
A
B
C
D_1
D_2

Scale setting t_0

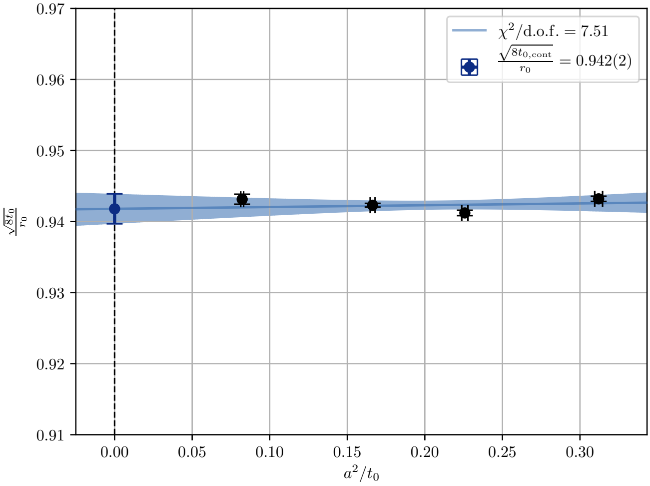

- The continuum extrapolation $a \to 0$ for t_0 of the four ensembles A, B, C, and D_2.

Scale setting t_0

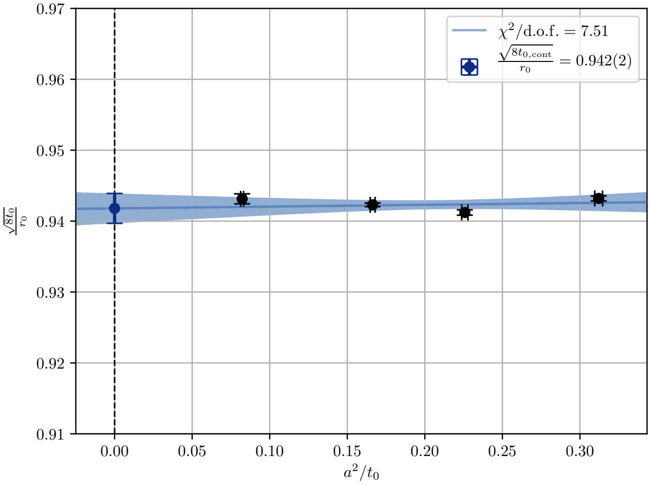

Continuum extrapolation using ensembles A, B, C, and D_2 gives $t_{0,\mathrm{cont}}/r_0^2 = 0.11087(50)$.

- The continuum extrapolation $a \to 0$ for t_0 of the four ensembles A, B, C, and D_2.
- $r_0 = 0.5$ fm.

Scale setting t_0

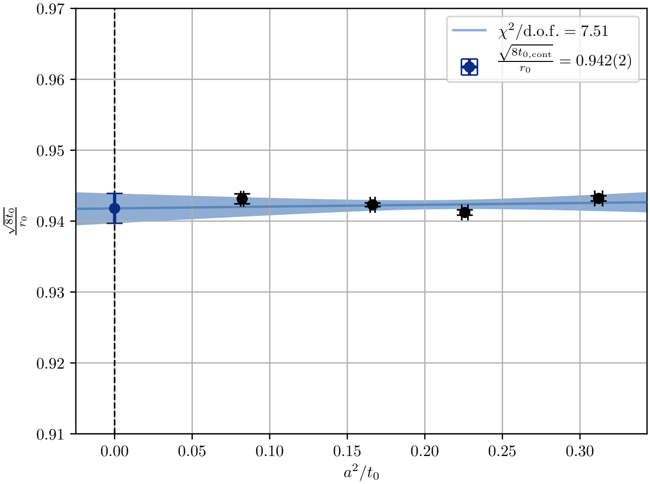

Continuum extrapolation using ensembles A, B, C, and D_2 gives $t_{0,\mathrm{cont}}/r_0^2 = 0.11087(50)$. This matches the values retrieved by Lüscher [3].

- The continuum extrapolation $a \to 0$ for t_0 of the four ensembles A, B, C, and D_2.
- $r_0 = 0.5$ fm.

Extrapolations for different ensemble-combinations

Ensembles	$t_{0,\mathrm{cont}}/r_0^2$	$\chi^2/\mathrm{d.o.f}$
A, B, C, D_2	$0.11087(50)$	7.51
B, C, D_2	$0.1115(3)$	0.41
A, B, C, D_1	$0.1119(6)$	0.88

- Notice the χ^2/d.o.f. of the extrapolation versus the two other extrapolations.

Scale setting w_0

Can also set a scale using the derivative which offers more granularity for small flow times,

$$
\begin{aligned}
W(t)|_{t=w_0^2} &= 0.3, \\
W(t) &\equiv t_f \frac{\mathrm{d}}{\mathrm{d}t_f} \left\{ t_f^2 \langle E \rangle \right\}.
\end{aligned}
$$

First presented by Borsanyi et al. [1].

Scale setting w_0

Ensembles	$w_{0,\mathrm{cont}}$[fm]	$\chi^2/\mathrm{d.o.f}$
A, B, C, D_2	$0.1695(5)$	7.12
B, C, D_2	$0.1702(3)$	0.53
A, B, C, D_1	$0.1706(6)$	0.86

Scale setting w_0

Ensembles	$w_{0,\mathrm{cont}}$[fm]	$\chi^2/\mathrm{d.o.f}$
A, B, C, D_2	$0.1695(5)$	7.12
B, C, D_2	$0.1702(3)$	0.53
A, B, C, D_1	$0.1706(6)$	0.86

Comparable to Borsanyi et al. [1] which included dynamical fermions, with $w_{0,\mathrm{cont}} = 0.1755(18)(04)$ fm.

Topological charge

- Gauge fields can be classified by their topological properties.

Topological charge

- Gauge fields can be classified by their topological properties.
- **Topological charge** Q can be viewed as a “measure” of instantons.

- Measuring **topological charge** is a measure of the *Winding number* of the gauge field.

Topological charge

- Gauge fields can be classified by their topological properties.
- **Topological charge** Q can be viewed as a “measure” of instantons.
- **Instantons** are local minimums of the Yang-Mills action in Euclidean space.

- Measuring **topological charge** is a measure of the *Winding number* of the gauge field.
- **Instantons** are local minimums to the Yang-Mills action in Euclidean space.
- Instantons are significant in LQCD because of *critical slowdown* which we will return to later.

- Gauge fields can be classified by their topological properties.
- **Topological charge** Q can be viewed as a "measure" of instantons.
- **Instantons** are local minimums of the Yang-Mills action in Euclidean space.

$$Q = a^4 \sum_{n\in\Lambda} q(n),$$

with the charge density given by

$$q(n) = \frac{1}{32\pi^2}\epsilon_{\mu\nu\rho\sigma}\mathrm{tr}\left[F_{\mu\nu}(n)F_{\rho\sigma}(n)\right].$$

- Measuring **topological charge** is a measure of the *Winding number* of the gauge field.
- **Instantons** are local minimums to the Yang-Mills action in Euclidean space.
- Instantons are significant in LQCD because of *critical slowdown* which we will return to later.
- The charge is a **sum over the local charge** at every point in the gauge field.
- Can in a very crude manner be viewed as the "curl" of the gauge fields.

Topological charge

- Gauge fields can be classified by their topological properties.
- **Topological charge** Q can be viewed as a "measure" of instantons.
- **Instantons** are local minimums of the Yang-Mills action in Euclidean space.

$$Q = a^4 \sum_{n \in \Lambda} q(n),$$

with the charge density given by

$$q(n) = \frac{1}{32\pi^2} \epsilon_{\mu\nu\rho\sigma} \mathrm{tr}\left[F_{\mu\nu}(n) F_{\rho\sigma}(n)\right].$$

$$\langle Q \rangle = 0$$

- Measuring **topological charge** is a measure of the *Winding number* of the gauge field.
- **Instantons** are local minimums to the Yang-Mills action in Euclidean space.
- Instantons are significant in LQCD because of *critical slowdown* which we will return to later.
- The charge is a **sum over the local charge** at every point in the gauge field.
- Can in a very crude manner be viewed as the "curl" of the gauge fields.
- The **expectation value** of Q **is zero** due to it being **parity odd**.

- Gauge fields can be classified by their topological properties.
- **Topological charge** Q can be viewed as a “measure” of instantons.
- **Instantons** are local minimums of the Yang-Mills action in Euclidean space.

$$Q = a^4 \sum_{n \in \Lambda} q(n),$$

with the charge density given by

$$q(n) = \frac{1}{32\pi^2} \epsilon_{\mu\nu\rho\sigma} \mathrm{tr}\left[F_{\mu\nu}(n) F_{\rho\sigma}(n)\right].$$

$$\langle Q \rangle = 0$$

- Measuring **topological charge** is a measure of the *Winding number* of the gauge field.
- **Instantons** are local minimums to the Yang-Mills action in Euclidean space.
- Instantons are significant in LQCD because of *critical slowdown* which we will return to later.
- The charge is a **sum over the local charge** at every point in the gauge field.
- Can in a very crude manner be viewed as the “curl” of the gauge fields.
- The **expectation value** of Q **is zero** due to it being **parity odd**.

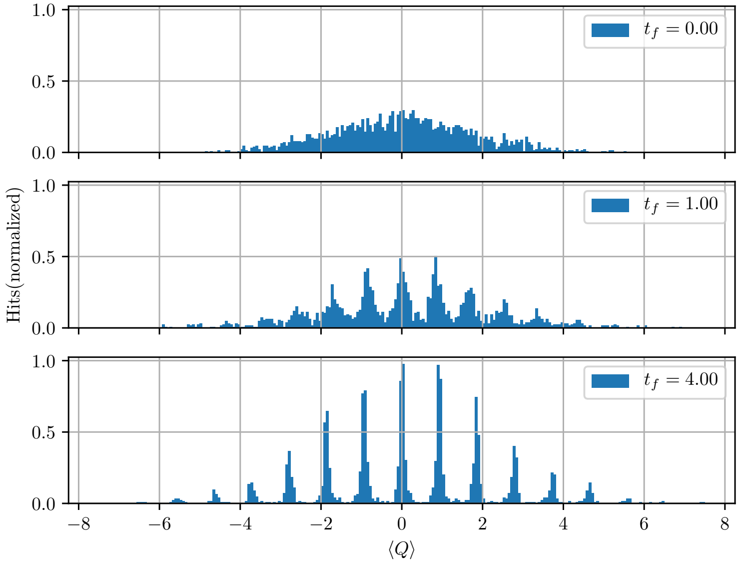

Histograms for the Q for ensemble G with a lattice of size $N^3 \times N_T = 16^3 \times 32$ with $\beta = 6.1$, taken at different flow times $t_f/a^2 = 0.0$, 1.0, 4.0 fm.

Topological charge distribution in flow time

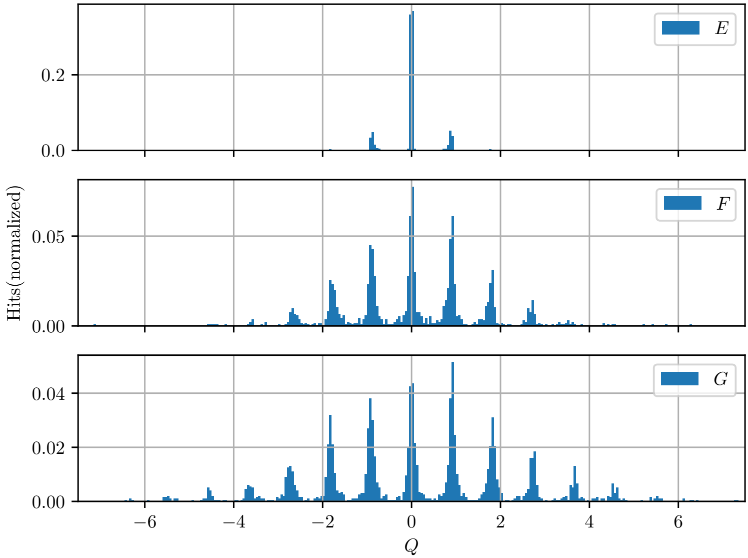

Histograms of topological charge for the supporting ensembles seen at $t_f/a^2 = 0.25$ fm.

Topological charge for our main ensembles

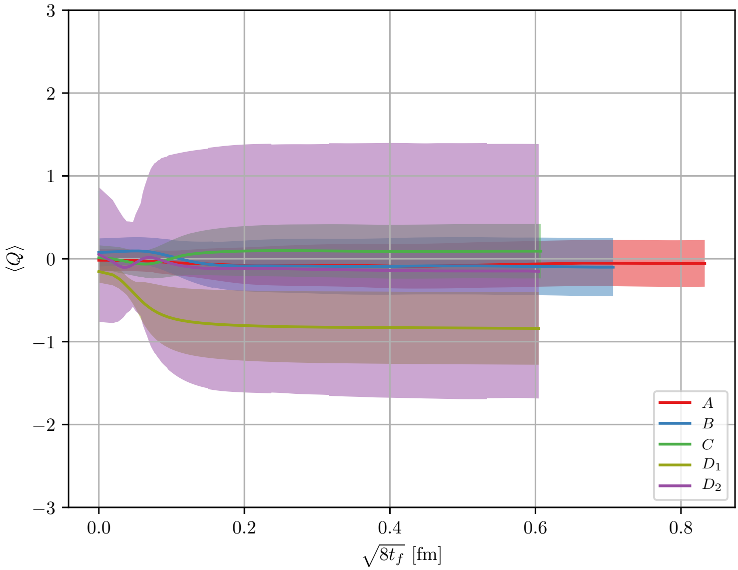

Why is the charge not centered around zero for certain ensembles?

Autocorrelation in the energy

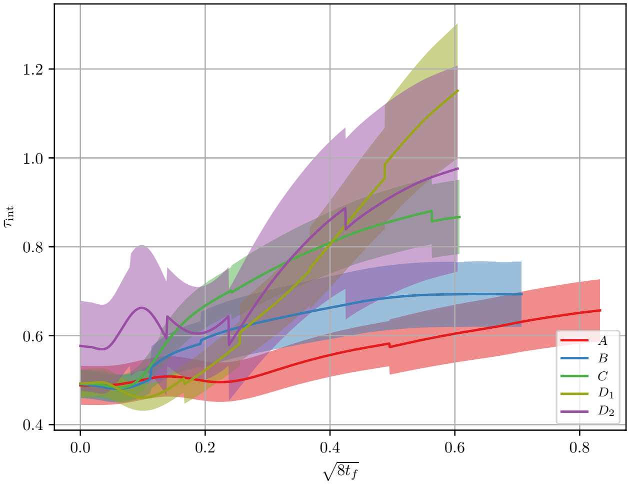

The autocorrelation of the energy. A value of $\tau_{\mathrm{int}} = 0.5$ indicates that we have zero autocorrelation.

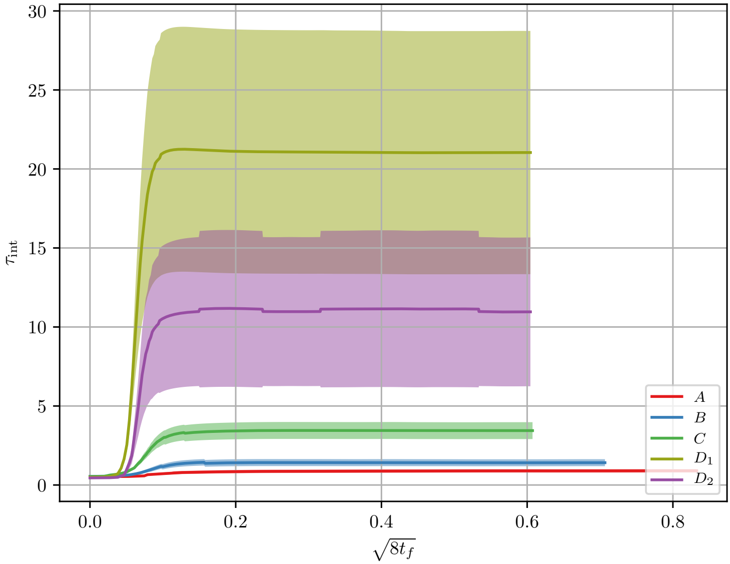

- The integrated autocorrelation $\tau_{\rm int}$ for topological charge for the five main ensembles.

Critical slowdown

Critical slowdown is the phenomena where we as the lattice spacing a *decreases* the required energy to tunnel from one state to another *increase*.

Critical slowdown

Critical slowdown is the phenomena where we as the lattice spacing a *decreases* the required energy to tunnel from one state to another *increase*.
$\rightarrow$ many more lattice updates are required in order to have independent gauge configurations.

- That is, going from one instanton sector to another requires many more updates and becomes an inherent problem in all LQCD calculations.

Critical slowdown is the phenomena where we as the lattice spacing a *decreases* the required energy to tunnel from one state to another *increase*.
$\rightarrow$ many more lattice updates are required in order to have independent gauge configurations.

- That is, going from one instanton sector to another requires many more updates and becomes an inherent problem in all LQCD calculations.
- In the continuum it would require an **infinite amount of energy** to go from **one instanton sector to another**. Thus as we a **approaches the continuum**, the amount of **effort**(number of updates ect.) required to generate **independent** gauge configurations **increases**.

Critical slowdown

Critical slowdown is the phenomena where we as the lattice spacing a *decreases* the required energy to tunnel from one state to another *increase*.
$\rightarrow$ many more lattice updates are required in order to have independent gauge configurations.

- That is, going from one instanton sector to another requires many more updates and becomes an inherent problem in all LQCD calculations.
- In the continuum it would require an **infinite amount of energy** to go from **one instanton sector to another**. Thus as we a **approaches the continuum**, the amount of **effort**(number of updates ect.) required to generate **independent** gauge configurations **increases**.

Topological susceptibility

The *topological susceptibility* is given by

$$\chi_{\text{top}}^{1/4} = \frac{1}{V^{1/4}} \left\langle Q^2 \right\rangle^{1/4}$$

with V being the lattice volume and $\left\langle Q^2 \right\rangle$ is the second momenta of the charge.

Topological susceptibility

The *topological susceptibility* is given by

$$\chi_{\text{top}}^{1/4} = \frac{1}{V^{1/4}} \left\langle Q^2 \right\rangle^{1/4}$$

with V being the lattice volume and $\left\langle Q^2 \right\rangle$ is the second momenta of the charge.

The *Witten-Veneziano relation* is given by

$$m_{\eta'}^2 = \frac{2N_f}{f_\pi^2} \chi_{\text{top}}$$

- R.h.s. is full QCD and l.h.s is from pure gauge theory.

The *topological susceptibility* is given by

$$\chi_{\text{top}}^{1/4} = \frac{1}{V^{1/4}} \left\langle Q^2 \right\rangle^{1/4}$$

with V being the lattice volume and $\left\langle Q^2 \right\rangle$ is the second momenta of the charge.

The *Witten-Veneziano relation* is given by

$$m_{\eta'}^2 = \frac{2N_f}{f_\pi^2} \chi_{\text{top}}$$

with

- pion decay constant $f_\pi = 0.130(5)/\sqrt{2}$ GeV.

- R.h.s. is full QCD and l.h.s is from pure gauge theory.
- We can use the Witten-Veneziano formula in order to extract an estimate for N_f using the topological susceptibility.

Topological susceptibility

The *topological susceptibility* is given by

$$\chi_{\text{top}}^{1/4} = \frac{1}{V^{1/4}} \left\langle Q^2 \right\rangle^{1/4}$$

with V being the lattice volume and $\left\langle Q^2 \right\rangle$ is the second momenta of the charge.
The *Witten-Veneziano relation* is given by

$$m_{\eta'}^2 = \frac{2N_f}{f_\pi^2} \chi_{\text{top}}$$

with

- pion decay constant $f_\pi = 0.130(5)/\sqrt{2}$ GeV.
- η' meson mass $m_{\eta'} = 0.95778(6)$ GeV.

- R.h.s. is full QCD and l.h.s is from pure gauge theory.
- We can use the Witten-Veneziano formula in order to extract an estimate for N_f using the topological susceptibility.

The *topological susceptibility* is given by

$$\chi_{\mathrm{top}}^{1/4} = \frac{1}{V^{1/4}} \left\langle Q^2 \right\rangle^{1/4}$$

with V being the lattice volume and $\left\langle Q^2 \right\rangle$ is the second momenta of the charge.

The *Witten-Veneziano relation* is given by

$$m_{\eta'}^2 = \frac{2N_f}{f_\pi^2} \chi_{\mathrm{top}}$$

with

- pion decay constant $f_\pi = 0.130(5)/\sqrt{2}$ GeV.
- η' meson mass $m_{\eta'} = 0.95778(6)$ GeV.
- N_f is the number of flavors(i.e. quark species involved in η'.).

- R.h.s. is full QCD and l.h.s is from pure gauge theory.
- We can use the Witten-Veneziano formula in order to extract an estimate for N_f using the topological susceptibility.

Topological susceptibility

The *topological susceptibility* is given by

$$\chi_{\text{top}}^{1/4} = \frac{1}{V^{1/4}} \left\langle Q^2 \right\rangle^{1/4}$$

with V being the lattice volume and $\left\langle Q^2 \right\rangle$ is the second momenta of the charge.
The *Witten-Veneziano relation* is given by

$$m_{\eta'}^2 = \frac{2N_f}{f_\pi^2} \chi_{\text{top}}$$

with

- pion decay constant $f_\pi = 0.130(5)/\sqrt{2}$ GeV.
- η' meson mass $m_{\eta'} = 0.95778(6)$ GeV.
- N_f is the number of flavors(i.e. quark species involved in η'.).

We expect $N_f = 3$.

- R.h.s. is full QCD and l.h.s is from pure gauge theory.
- We can use the Witten-Veneziano formula in order to extract an estimate for N_f using the topological susceptibility.
- This can help us understand the ”quality” of the ensemble, as we would expect to be around $N_f = 3$.

Topological susceptibility

The *topological susceptibility* is given by

$$\chi_{\text{top}}^{1/4} = \frac{1}{V^{1/4}} \left\langle Q^2 \right\rangle^{1/4}$$

with V being the lattice volume and $\left\langle Q^2 \right\rangle$ is the second momenta of the charge.

The *Witten-Veneziano relation* is given by

$$m_{\eta'}^2 = \frac{2N_f}{f_\pi^2} \chi_{\text{top}}$$

with

- pion decay constant $f_\pi = 0.130(5)/\sqrt{2}$ GeV.
- η' meson mass $m_{\eta'} = 0.95778(6)$ GeV.
- N_f is the number of flavors(i.e. quark species involved in η'.).

We expect $N_f = 3$.

- R.h.s. is full QCD and l.h.s is from pure gauge theory.
- We can use the Witten-Veneziano formula in order to extract an estimate for N_f using the topological susceptibility.
- This can help us understand the ”quality” of the ensemble, as we would expect to be around $N_f = 3$.

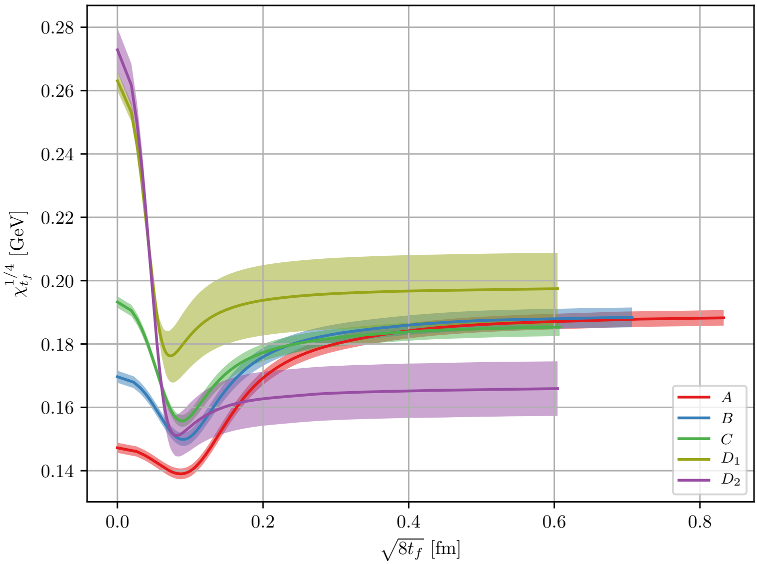

- The topological susceptibility $\chi_{t_f}^{1/4}$ of the **main ensembles**.
- We have a **UV divergence at zeroth flow time**, hence to need for gradient flow which renormalizes this quantity.
- **Bootstrapped** $N_{\mathrm{bs}} = 500$ times.
- **Corrected for autocorrelations** with $\sigma = \sqrt{2\tau_{\mathrm{int}}}\sigma_0$.

Topological susceptibility continuum extrapolation

Ensemble	$\chi_{t_f}^{1/4}$ [GeV]	$\chi_{t_f}^{1/4}$ [GeV], corrected	$\sqrt{2\tau_{\mathrm{int}}}$
A	$0.1877(23)$	$0.1877(24)$	$1.028(46)$
B	$0.1880(21)$	$0.1880(29)$	$1.346(81)$
C	$0.1853(14)$	$0.1853(24)$	$1.762(104)$
D_1	$0.1971(22)$	$0.1971(101)$	$4.523(675)$
D_2	$0.1656(33)$	$0.1656(86)$	$2.624(441)$

Error corrected for autocorrelations with $\sigma = \sqrt{2\tau_{\mathrm{int}}}\sigma_0$.
Values taken at $\sqrt{8t_f} = 0.6$ fm.

- Values extracted at a smearing radius of **hadronic scales**. That is, we have plateaued and have no discretization effects.
- The topological susceptibility for the main ensembles together with the correction factor from the integrated autocorrelation time. The second column have not had its results corrected by $\sqrt{2\tau_{\mathrm{int}}}$. None of the results have been analyzed with bootstrapping.

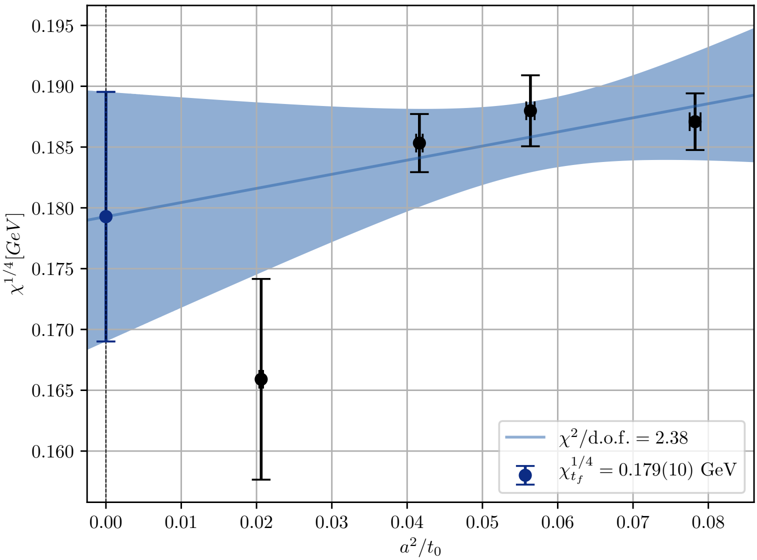

- A continuum extrapolation of the topological susceptibility $\chi_{t_f}^{1/4}$ for the main ensembles excluding the D_1 ensemble.
- The points for $\chi_{t_f}^{1/4}$ is taken at $\sqrt{8t_{f,0}} = 0.6$ fm.

Topological susceptibility continuum extrapolation

Ensembles	$\chi_{t_f}^{1/4}$ $(\langle Q^2 \rangle)$ [GeV]	N_f	$\chi^2/\mathrm{d.o.f}$
A, B, C, D_2	$0.179(10)$	$3.75(29)$	2.38
A, B, C, D_1	$0.186(6)$	$3.21(25)$	0.83
B, C, D_1	$0.187(24)$	$3.18(24)$	1.63
B, C, D_2	$0.166(24)$	$5.06(39)$	2.05
A, B, C	$0.184(6)$	$3.37(26)$	0.33

The fourth cumulant

$$\left\langle Q^4 \right\rangle_c = \frac{1}{V^2}\left(\left\langle Q^4 \right\rangle - 3\left\langle Q^2 \right\rangle^2 \right).$$

From this, we can also measure the ratio R,

$$R = \frac{\left\langle Q^4 \right\rangle_c}{\frac{1}{V}\left\langle Q^2 \right\rangle} = \frac{1}{V}\frac{\left\langle Q^4 \right\rangle - 3\left\langle Q^2 \right\rangle^2}{\left\langle Q^2 \right\rangle},$$

- Highly unstable, as we shall see.
- Will provide insight into the goodness of our ensembles.
- An R-value away from 1 will indicate that QCD cannot be described by the dilute instanton gas model.

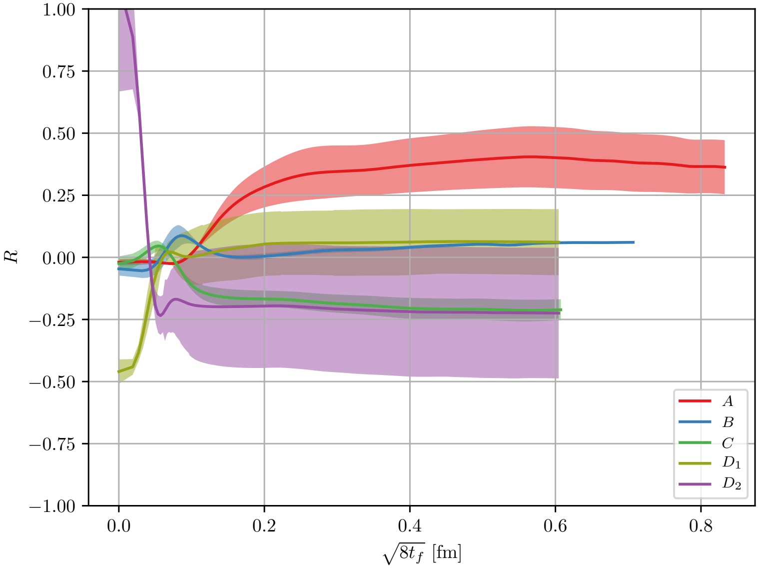

- The fourth cumulant ratio $R = \left\langle Q^4 \right\rangle_C / \left\langle Q^2 \right\rangle$.
- The results was analyzed using $N_{\mathrm{bs}} = 500$ bootstrap samples, with the error corrected for by $\sqrt{2\tau_{\mathrm{int}}}$.

The fourth cumulant at reference flow times

Ensemble	L/a	t_0/a^2	$\langle Q^2 \rangle$	$\langle Q^4 \rangle$	$\langle Q^4 \rangle_C$	R
A	2.24	$3.20(3)$	$0.78(4)$	$2.13(27)$	$0.282(67)$	$0.359(65)$
B	2.21	$4.43(4)$	$0.81(5)$	$1.98(23)$	$0.036(11)$	$0.044(11)$
C	2.17	$6.01(6)$	$0.77(4)$	$1.6(2)$	$-0.174(40)$	$-0.226(64)$
D_1	1.53	$12.2(1)$	$1.00(20)$	$3.01(1.07)$	$0.03(12)$	$0.03(12)$
D_2	2.29	$12.2(1)$	$0.497(100)$	$0.64(20)$	$-0.103(95)$	$-0.21(23)$

The fourth cumulant is taken at their individual reference scales seen in the third column. The data were analyzed with using a bootstrap analysis of $N_{bs} = 500$ samples, with error corrected by the integrated autocorrelation, $\sqrt{2\tau_{\text{int}}}$.

Comparing fourth cumulant

We can compare with article by Cè et al. [2]

Comparing fourth cumulant

Ensemble	β	L/a	L [fm]	a [fm]	t_0/a^2	t_0/r_0^2	N_{cfg}
F_1	5.96	16	1.632	0.102	2.7887(2)	0.1113(9)	1 440 000
B_2	6.05	14	1.218	0.087	3.7960(12)	0.1114(9)	144 000
$\tilde{D}_2$		17	1.479		3.7825(8)	0.1110(9)	
B_3	6.13	16	1.232	0.077	4.8855(15)	0.1113(10)	144 000
$\tilde{D}_3$		19	1.463		4.8722(11)	0.1110(10)	
B_4	6.21	18	1.224	0.068	6.2191(20)	0.1115(11)	144 000
$\tilde{D}_4$		21	1.428		6.1957(14)	0.1111(11)	

- Parameters of the ensembles presented by Cè et al. [2]. The first column is the ensemble name from the article. The letter indicates the volume, while the subindex indicates the β value. Ensembles of similar letters keep approximately the same length L.

Comparing fourth cumulant

Ensemble	$\langle Q^2 \rangle_{\text{normed}}$	$\langle Q^4 \rangle_{\text{normed}}$	$\langle Q^4 \rangle_{C,\text{normed}}$	R_{normed}
F_1	$0.728(1)$	$1.608(4)$	$0.016(1)$	$0.022(1)$
B_2	$0.772(3)$	$1.873(19)$	$0.085(4)$	$0.110(5)$
$\tilde{D}_2$	$0.770(3)$	$1.817(17)$	$0.037(4)$	$0.048(5)$
B_3	$0.760(3)$	$1.805(17)$	$0.074(3)$	$0.097(4)$
$\tilde{D}_3$	$0.769(3)$	$1.801(14)$	$0.027(1)$	$0.035(1)$
B_4	$0.776(3)$	$1.874(18)$	$0.069(3)$	$0.089(4)$
$\tilde{D}_4$	$0.785(3)$	$1.891(17)$	$0.040(4)$	$0.052(5)$

- Results as presented by Cè et al. [2], **normalized by the lattice volume**.

Comparing fourth cumulant

Article	Thesis	Ratio($\langle Q^2 \rangle$)	Ratio($\langle Q^4 \rangle$)	Ratio($\langle Q^4 \rangle_C$)	Ratio(R)
F_1	A	$1.08(6)$	$1.34(18)$	$19.03(5.81)$	$17.64(4.48)$
B_2	A	$1.02(5)$	$1.15(15)$	$3.60(1.09)$	$3.54(90)$
	B	$1.04(6)$	$1.06(11)$	$0.480(74)$	$0.46(4)$
$\tilde{D}_2$	A	$1.02(5)$	$1.19(15)$	$8.31(1.99)$	$8.15(1.56)$
	B	$1.05(6)$	$1.10(12)$	$1.1(1)$	$1.06(3)$
B_3	B	$1.06(6)$	$1.10(12)$	$0.550(86)$	$0.52(5)$
$\tilde{D}_3$	B	$1.05(6)$	$1.11(12)$	$1.51(23)$	$1.4(1)$
B_4	C	$0.99(5)$	$0.86(8)$	$-2.32(46)$	$-2.35(59)$
$\tilde{D}_4$	C	$0.98(5)$	$0.85(8)$	$-3.95(96)$	$-4.05(1.19)$

- A comparison between the results obtained in this thesis on the fourth cumulant, and by those similar in volume form Cè et al. [2]. *Ratio* indicates that we are dividing our results by the ones in previous table.

Comparing fourth cumulant

Article	Thesis	Ratio($\langle Q^2 \rangle$)	Ratio($\langle Q^4 \rangle$)	Ratio($\langle Q^4 \rangle_C$)	Ratio(R)
F_1	A	$1.08(6)$	$1.34(18)$	$19.03(5.81)$	$17.64(4.48)$
B_2	A	$1.02(5)$	$1.15(15)$	$3.60(1.09)$	$3.54(90)$
	B	$1.04(6)$	$1.06(11)$	$0.480(74)$	$0.46(4)$
$\tilde{D}_2$	A	$1.02(5)$	$1.19(15)$	$8.31(1.99)$	$8.15(1.56)$
	B	$1.05(6)$	$1.10(12)$	$1.1(1)$	$1.06(3)$
B_3	B	$1.06(6)$	$1.10(12)$	$0.550(86)$	$0.52(5)$
$\tilde{D}_3$	B	$1.05(6)$	$1.11(12)$	$1.51(23)$	$1.4(1)$
B_4	C	$0.99(5)$	$0.86(8)$	$-2.32(46)$	$-2.35(59)$
$\tilde{D}_4$	C	$0.98(5)$	$0.85(8)$	$-3.95(96)$	$-4.05(1.19)$

- A comparison between the results obtained in this thesis on the fourth cumulant, and by those similar in volume form Cè et al. [2]. *Ratio* indicates that we are dividing our results by the ones in previous table.

The **topological charge correlator**

$$C(n_t) = \langle q(n_t) q(0) \rangle \,,$$

$q(0)$ is the *source* placed at a fixed Euclidean time, and $q(n_t)$ is the *sink* which is summed across all Euclidean times.

- $q(0)$ is not required to be at $n_t = 0$.

The topological charge correlator

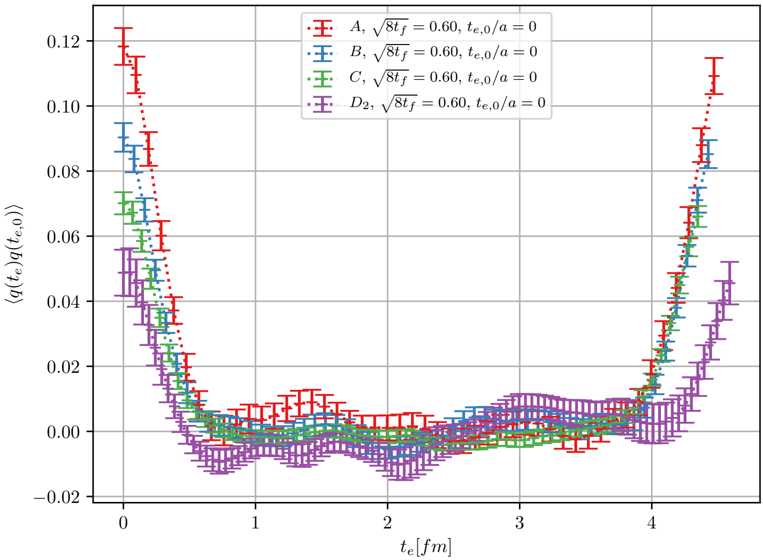

- The topological charge correlator for all of the ensembles except D_1. The x-axis contains the sink-source separation, as the source $q(0)$ is placed at $t_e = 0$ fm, and the sink $q(t_e)$ is taken at t_e.

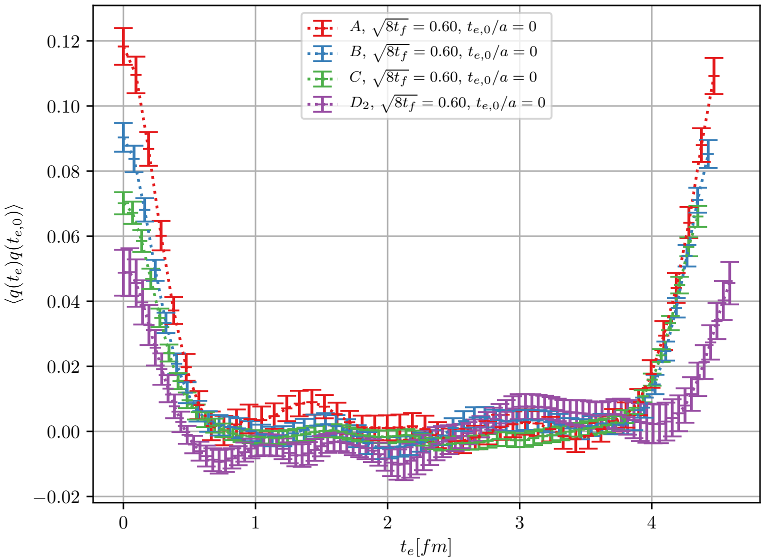

- The topological charge correlator for all of the ensembles except D_1. The x-axis contains the sink-source separation, as the source $q(0)$ is placed at $t_e = 0$ fm, and the sink $q(t_e)$ is taken at t_e.
- We since the ensembles are of different lattice sizes, we plot th D_1 separately.

The topological charge correlator

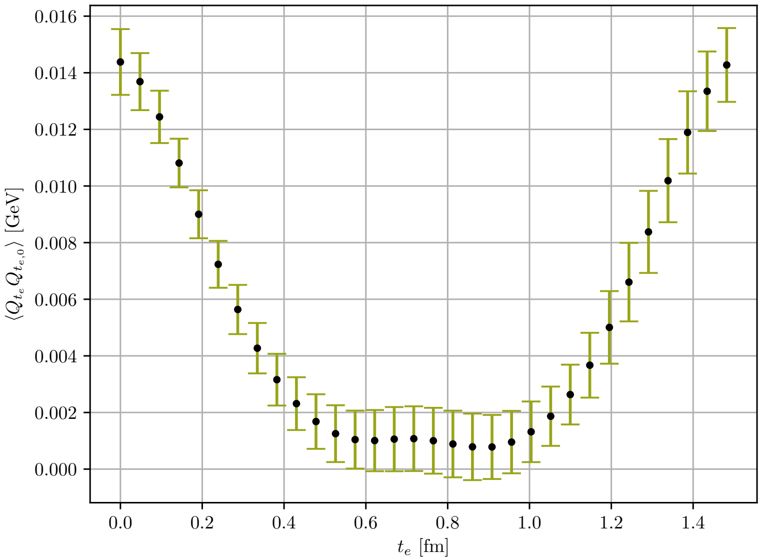

- The topological charge correlator for all of the ensembles except D_1. The x-axis contains the sink-source separation, as the source $q(0)$ is placed at $t_e = 0$ fm, and the sink $q(t_e)$ is taken at t_e.
- We since the ensembles are of different lattice sizes, we plot th D_1 separately.
- The topological charge correlator for the D_1. The source $q(0)$ is placed at $t_e = 0$ fm and the sink $q(t_e)$ is taken at t_e.

The topological charge correlator

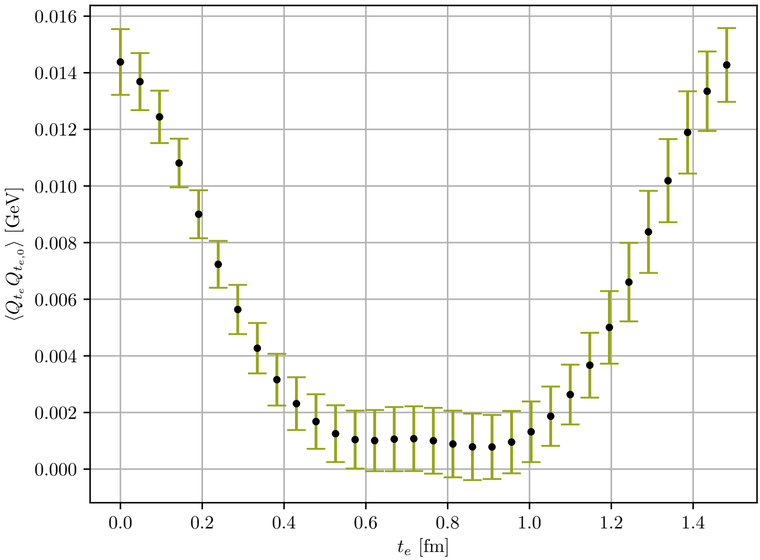

- The topological charge correlator for all of the ensembles except D_1. The x-axis contains the sink-source separation, as the source $q(0)$ is placed at $t_e = 0$ fm, and the sink $q(t_e)$ is taken at t_e.
- We since the ensembles are of different lattice sizes, we plot th D_1 separately.
- The topological charge correlator for the D_1. The source $q(0)$ is placed at $t_e = 0$ fm and the sink $q(t_e)$ is taken at t_e.
- We would expect an **exponential dampening**.

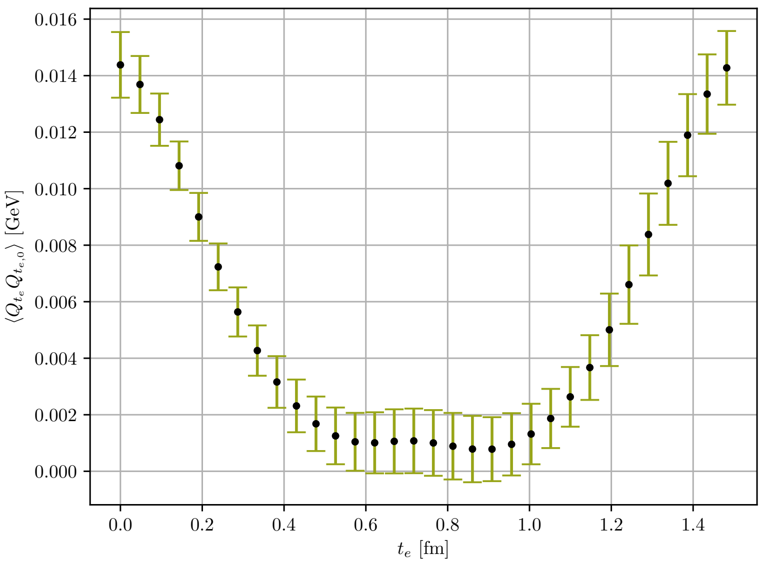

- The topological charge correlator for all of the ensembles except D_1. The x-axis contains the sink-source separation, as the source $q(0)$ is placed at $t_e = 0$ fm, and the sink $q(t_e)$ is taken at t_e.
- We since the ensembles are of different lattice sizes, we plot th D_1 separately.
- The topological charge correlator for the D_1. The source $q(0)$ is placed at $t_e = 0$ fm and the sink $q(t_e)$ is taken at t_e.
- We would expect an **exponential dampening**.

The effective glueball mass

A glueball is a bound state of gluons.

In pure Yang-Mills gauge theory, the states are stable.
We will be looking at the state involving topological charge.

The effective glueball mass

A glueball is a bound state of gluons.
The ground state in the correlator is given as

$$C(n_t) = A_0 \mathrm{e}^{-n_t E_0} + A_1 \mathrm{e}^{-n_t E_1} + \ldots$$

In pure Yang-Mills gauge theory, the states are stable.
We will be looking at the state involving topological charge.

The effective glueball mass

A glueball is a bound state of gluons.
The ground state in the correlator is given as

$$C(n_t) = A_0 \mathrm{e}^{-n_t E_0} + A_1 \mathrm{e}^{-n_t E_1} + \ldots$$

which can be extracted as

$$am_{\text{eff}} = \log\left(\frac{C(n_t)}{C(n_t+1)}\right),$$

In pure Yang-Mills gauge theory, the states are stable.
We will be looking at the state involving topological charge.

The effective glueball mass

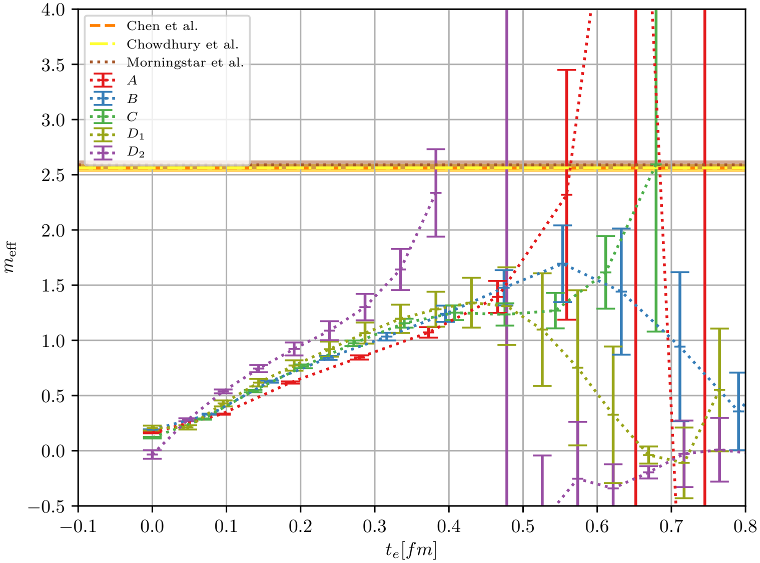

- The effective mass of the glueball, as extracted from the topological charge correlator in Euclidean time.

The effective glueball mass

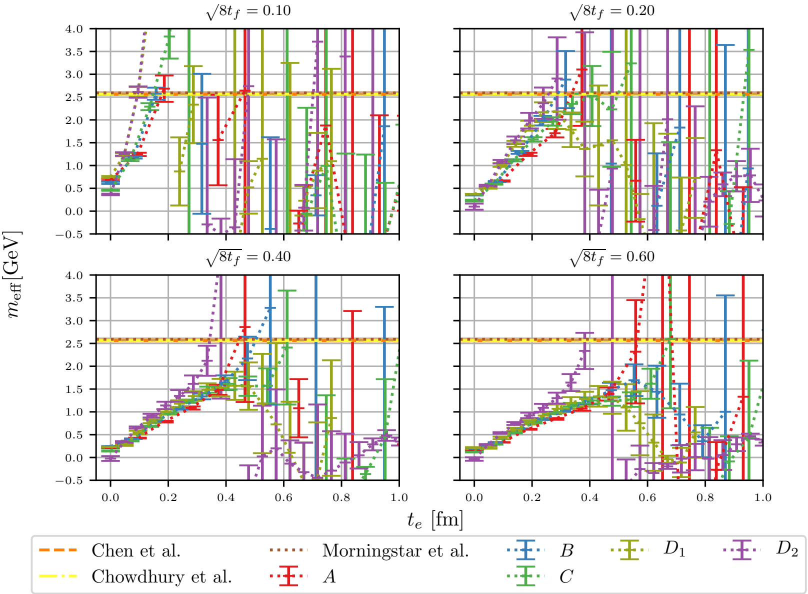

- The effective mass of the glueball, as extracted from the topological charge correlator in Euclidean time.
- Low statistics and critical slowdown → poor signal.

The effective glueball mass

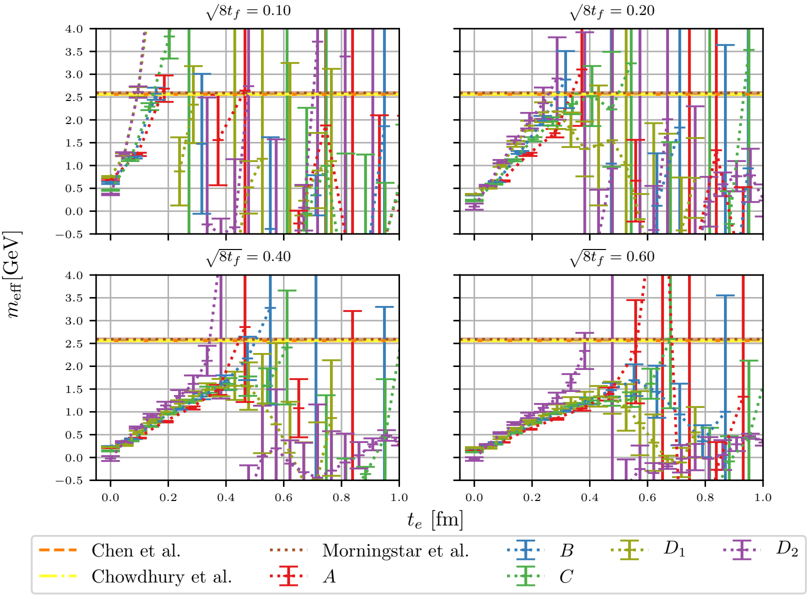

- The effective mass of the glueball, as extracted from the topological charge correlator in Euclidean time.
- Low statistics and critical slowdown → poor signal.

Conclusion, future developments and final thoughts

Conclusion

- Created a code capable of generating and flowing gauge configurations.

- Checked scaling and parameter optimization.

Conclusion

- Created a code capable of generating and flowing gauge configurations.
  - Verified to match other code bases down to machine precision.

- Checked scaling and parameter optimization.
- Same results as Chroma down to machine precision.

- Created a code capable of generating and flowing gauge configurations.
  - Verified to match other code bases down to machine precision.
- t_0 and w_0 match other papers, e.g. Lüscher [3] and Cè et al. [2].

- Checked scaling and parameter optimization.
- Same results as Chroma down to machine precision.
- t_0 and w_0 match other papers.

- Created a code capable of generating and flowing gauge configurations.
  - Verified to match other code bases down to machine precision.
- t_0 and w_0 match other papers, e.g. Lüscher [3] and Cè et al. [2].
- $\langle Q \rangle \neq 0$ for some ensembles.

- Checked scaling and parameter optimization.
- Same results as Chroma down to machine precision.
- t_0 and w_0 match other papers.
- $\langle Q \rangle$

- Created a code capable of generating and flowing gauge configurations.
  - Verified to match other code bases down to machine precision.
- t_0 and w_0 match other papers, e.g. Lüscher [3] and Cè et al. [2].
- $\langle Q \rangle \neq 0$ for some ensembles.
- The topological susceptibility $\left\langle \chi_f^{1/4} \right\rangle$ and N_f

- Checked scaling and parameter optimization.
- Same results as Chroma down to machine precision.
- t_0 and w_0 match other papers.
- $\langle Q \rangle$
- $\chi_f^{1/4}$. Matches well with other papers

Conclusion

- Created a code capable of generating and flowing gauge configurations.
  - Verified to match other code bases down to machine precision.
- t_0 and w_0 match other papers, e.g. Lüscher [3] and Cè et al. [2].
- $\langle Q \rangle \neq 0$ for some ensembles.
- The topological susceptibility $\left\langle \chi_f^{1/4} \right\rangle$ and N_f
- $\left\langle Q^4 \right\rangle_C$ and R. Sensitive quantities - need large statistics.

- Checked scaling and parameter optimization.
- Same results as Chroma down to machine precision.
- t_0 and w_0 match other papers.
- $\langle Q \rangle$
- $\chi_f^{1/4}$. Matches well with other papers
- $\left\langle Q^4 \right\rangle_C$ and R. Sensitive quantity, matches well of first and second moment.

Conclusion

- Created a code capable of generating and flowing gauge configurations.
  - Verified to match other code bases down to machine precision.
- t_0 and w_0 match other papers, e.g. Lüscher [3] and Cè et al. [2].
- $\langle Q \rangle \neq 0$ for some ensembles.
- The topological susceptibility $\left\langle \chi_f^{1/4} \right\rangle$ and N_f
- $\left\langle Q^4 \right\rangle_C$ and R. Sensitive quantities - need large statistics.
- Topological charge correlator $\langle q(n_t) q(0) \rangle$ and glueball mass.

- Checked scaling and parameter optimization.
- Same results as Chroma down to machine precision.
- t_0 and w_0 match other papers.
- $\langle Q \rangle$
- $\chi_f^{1/4}$. Matches well with other papers
- $\left\langle Q^4 \right\rangle_C$ and R. Sensitive quantity, matches well of first and second moment.
- Topological charge correlator $\langle q(n_t) q(0) \rangle$ and glueball mass.

Conclusion

- Created a code capable of generating and flowing gauge configurations.
  - Verified to match other code bases down to machine precision.
- t_0 and w_0 match other papers, e.g. Lüscher [3] and Cè et al. [2].
- $\langle Q \rangle \neq 0$ for some ensembles.
- The topological susceptibility $\left\langle \chi_f^{1/4} \right\rangle$ and N_f
- $\left\langle Q^4 \right\rangle_C$ and R. Sensitive quantities - need large statistics.
- Topological charge correlator $\langle q(n_t) q(0) \rangle$ and glueball mass.
- Statistics, autocorrelation and critical slowdown.

- Checked scaling and parameter optimization.
- Same results as Chroma down to machine precision.
- t_0 and w_0 match other papers.
- $\langle Q \rangle$
- $\chi_f^{1/4}$. Matches well with other papers
- $\left\langle Q^4 \right\rangle_C$ and R. Sensitive quantity, matches well of first and second moment.
- Topological charge correlator $\langle q(n_t) q(0) \rangle$ and glueball mass.
- Critical slowdown, which makes transitioning to a new, independent configuration difficult. This inhibits the gathering of statistics, and helps us explain why we for larger β values have fewer independent gauge configurations.

- Created a code capable of generating and flowing gauge configurations.
    - Verified to match other code bases down to machine precision.
- t_0 and w_0 match other papers, e.g. Lüscher [3] and Cè et al. [2].
- $\langle Q \rangle \neq 0$ for some ensembles.
- The topological susceptibility $\left\langle \chi_f^{1/4} \right\rangle$ and N_f
- $\left\langle Q^4 \right\rangle_C$ and R. Sensitive quantities - need large statistics.
- Topological charge correlator $\langle q(n_t) q(0) \rangle$ and glueball mass.
- Statistics, autocorrelation and critical slowdown.

- Checked scaling and parameter optimization.
- Same results as Chroma down to machine precision.
- t_0 and w_0 match other papers.
- $\langle Q \rangle$
- $\chi_f^{1/4}$. Matches well with other papers
- $\left\langle Q^4 \right\rangle_C$ and R. Sensitive quantity, matches well of first and second moment.
- Topological charge correlator $\langle q(n_t) q(0) \rangle$ and glueball mass.
- Critical slowdown, which makes transitioning to a new, independent configuration difficult. This inhibits the gathering of statistics, and helps us explain why we for larger β values have fewer independent gauge configurations.

Future developments and final thoughts

- Better statistics - more gauge configurations.

Future developments and final thoughts

- Better statistics - more gauge configurations.
- Better utilization of support ensembles E, F and G.

Future developments and final thoughts

- Better statistics - more gauge configurations.
- Better utilization of support ensembles E, F and G.
- Improve autocorrelation with more updates per single link(increase N_{up}).

Future developments and final thoughts

- Better statistics - more gauge configurations.
- Better utilization of support ensembles E, F and G.
- Improve autocorrelation with more updates per single link(increase N_{up}).
- Implement better actions with operators that has smaller error contributions.

Future developments and final thoughts

- Better statistics - more gauge configurations.
- Better utilization of support ensembles E, F and G.
- Improve autocorrelation with more updates per single link(increase N_{up}).
- Implement better actions with operators that has smaller error contributions.
- Fermions and HMC(Hybrid Monte Carlo).

Questions?

References

[1] S. Borsanyi, S. Durr, Z. Fodor, C. Hoelbling, S. D. Katz, S. Krieg, T. Kurth, L. Lellouch, T. Lippert, C. McNeile, and K. K. Szabo. High-precision scale setting in lattice QCD. *Journal of High Energy Physics*, 2012(9), September 2012. ISSN 1029-8479. doi: 10.1007/JHEP09(2012)010. URL `http://arxiv.org/abs/1203.4469`. arXiv: 1203.4469.

[2] Marco Cè, Cristian Consonni, Georg P. Engel, and Leonardo Giusti. Non-Gaussianities in the topological charge distribution of the SU(3) Yang–Mills theory. *Physical Review D*, 92(7), October 2015. ISSN 1550-7998, 1550-2368. doi: 10.1103/PhysRevD.92.074502. URL `http://arxiv.org/abs/1506.06052`. arXiv: 1506.06052.

[3] Martin Lüscher. Properties and uses of the Wilson flow in lattice QCD. *Journal of High Energy Physics*, 2010(8), August 2010. ISSN 1029-8479. doi: 10.1007/JHEP08(2010)071. URL `http://arxiv.org/abs/1006.4518`. arXiv: 1006.4518.

Extras

Scaling

We checked three types of scaling,

- **Strong scaling:** *fixed problem* and a *variable N_p cores*

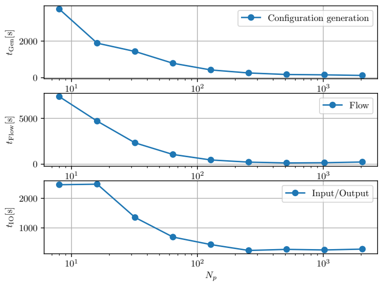

- Strong scaling

Scaling

We checked three types of scaling,

- **Strong scaling:** *fixed problem* and a *variable N_p cores*
- **Weak scaling:** *fixed problem per processor* and a *variable N_p cores.*

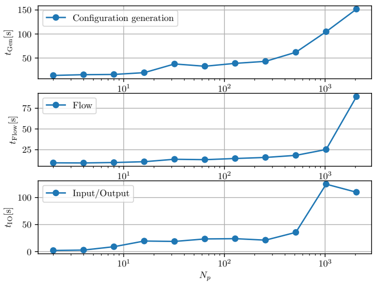

- Strong scaling
- Weak scaling

We checked three types of scaling,

- **Strong scaling:** *fixed problem* and a *variable N_p cores*
- **Weak scaling:** *fixed problem per processor* and a *variable N_p cores.*
- **Speedup:** defined as $S(p) = \frac{t_{N_p}}{t_{N_p,0}}$.

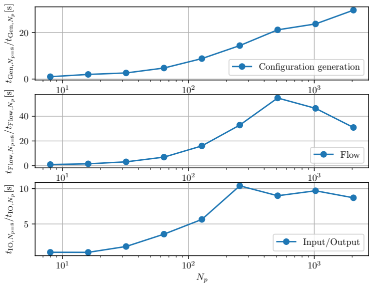

- Strong scaling
- Weak scaling
- The speedup of the configuration generation, flowing, and IO. The speedup is calculated by dividing the run time of each N_p run, with the run time of the run with the least number of processors, $N_p = 8$.

Scaling

We checked three types of scaling,

- **Strong scaling:** *fixed problem* and a *variable N_p cores*
- **Weak scaling:** *fixed problem per processor* and a *variable N_p cores*.
- **Speedup:** defined as $S(p) = \frac{t_{N_p}}{t_{N_p,0}}$.

- Strong scaling
- Weak scaling
- The speedup of the configuration generation, flowing, and IO. The speedup is calculated by dividing the run time of each N_p run, with the run time of the run with the least number of processors, $N_p = 8$.
- The IO was optimized later to be a factor of ten or more faster.

Scaling

We checked three types of scaling,

- **Strong scaling:** *fixed problem* and a *variable N_p cores*
- **Weak scaling:** *fixed problem per processor* and a *variable N_p cores*.
- **Speedup:** defined as $S(p) = \frac{t_{N_p}}{t_{N_p,0}}$.

We appear to have a plateau around 512 cores.

- Strong scaling
- Weak scaling
- The speedup of the configuration generation, flowing, and IO. The speedup is calculated by dividing the run time of each N_p run, with the run time of the run with the least number of processors, $N_p = 8$.
- The IO was optimized later to be a factor of ten or more faster.

Generated 200 configurations for a lattice of size $N^3 \times N_T = 16^3 \times 32$ and $\beta = 6.0$, for combinations of $N_{\mathrm{corr}} \in [200, 400, 600]$ and $N_{\mathrm{up}} \in [10, 20, 30]$.

- We run for different values for N_{up} and N_{corr} to see what gives optimizes **computational cost** and **autocorrelation**.
- The integrated autocorrelation time for topological charge $\langle Q \rangle$ for a lattice of size $N = 16$ and $N_T = 32$ with $\beta = 6.0$ for combinations of $N_{\mathrm{corr}} \in [200, 400, 600]$ and $N_{\mathrm{up}} \in [10, 20, 30]$, plotted against flow time $\sqrt{8t_f}$.

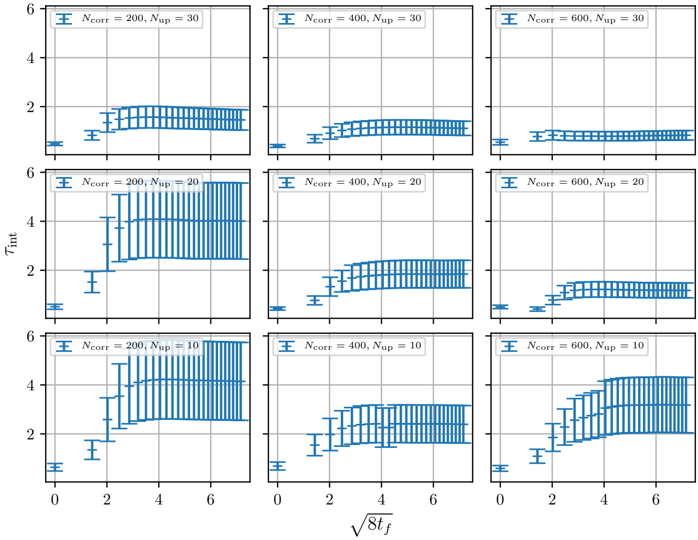

- We run for different values for N_{up} and N_{corr} to see what gives optimizes **computational cost** and **autocorrelation**.
- The integrated autocorrelation time for topological charge $\langle Q \rangle$ for a lattice of size $N = 16$ and $N_T = 32$ with $\beta = 6.0$ for combinations of $N_{\mathrm{corr}} \in [200, 400, 600]$ and $N_{\mathrm{up}} \in [10, 20, 30]$, plotted against flow time $\sqrt{8t_f}$.
- The time taking to generate 200 configurations and flowing them $N_{\mathrm{flow}} = 250$ flow steps for a lattice of size $N = 16$ and $N_T = 32$, with $\beta = 6.0$ for combinations of $N_{\mathrm{corr}} \in [200, 400, 600]$ and $N_{\mathrm{up}} \in [10, 20, 30]$.

Optimizing the gauge configuration generation

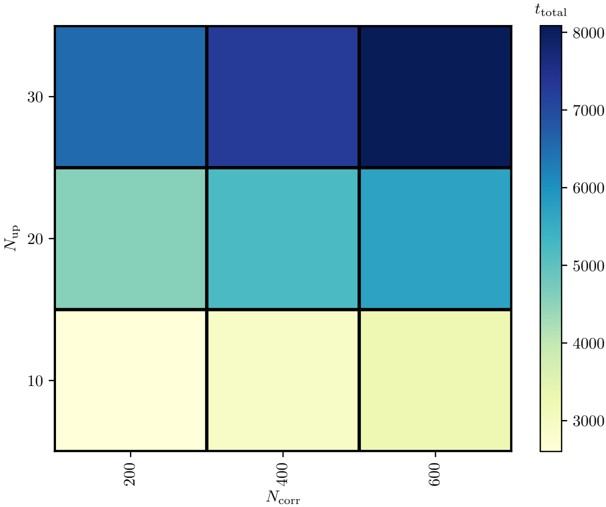

- We run for different values for N_{up} and N_{corr} to see what gives optimizes **computational cost** and **autocorrelation**.
- The integrated autocorrelation time for topological charge $\langle Q \rangle$ for a lattice of size $N = 16$ and $N_T = 32$ with $\beta = 6.0$ for combinations of $N_{\text{corr}} \in [200, 400, 600]$ and $N_{\text{up}} \in [10, 20, 30]$, plotted against flow time $\sqrt{8t_f}$.
- The time taking to generate 200 configurations and flowing them $N_{\text{flow}} = 250$ flow steps for a lattice of size $N = 16$ and $N_T = 32$, with $\beta = 6.0$ for combinations of $N_{\text{corr}} \in [200, 400, 600]$ and $N_{\text{up}} \in [10, 20, 30]$.
- What we see is that increasing N_{up} is a cheaper alternative compared to using N_{corr}

Optimizing the gauge configuration generation

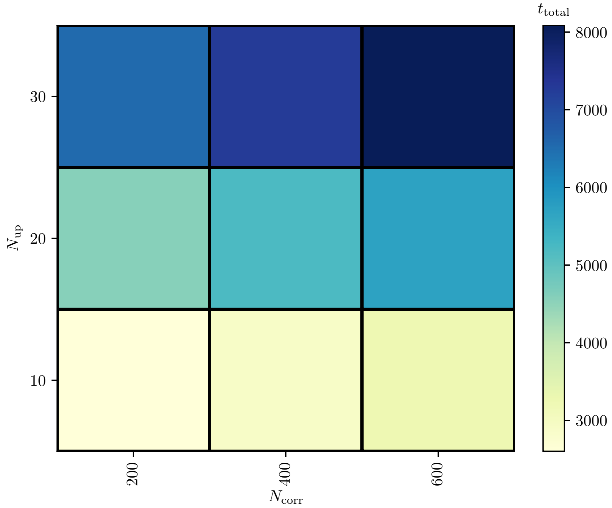

- We run for different values for N_{up} and N_{corr} to see what gives optimizes **computational cost** and **autocorrelation**.
- The integrated autocorrelation time for topological charge $\langle Q \rangle$ for a lattice of size $N = 16$ and $N_T = 32$ with $\beta = 6.0$ for combinations of $N_{\text{corr}} \in [200, 400, 600]$ and $N_{\text{up}} \in [10, 20, 30]$, plotted against flow time $\sqrt{8t_f}$.
- The time taking to generate 200 configurations and flowing them $N_{\text{flow}} = 250$ flow steps for a lattice of size $N = 16$ and $N_T = 32$, with $\beta = 6.0$ for combinations of $N_{\text{corr}} \in [200, 400, 600]$ and $N_{\text{up}} \in [10, 20, 30]$.
- What we see is that increasing N_{up} is a cheaper alternative compared to using N_{corr}

Verifying the code

- **Unit testing.** $\mathrm{SU}(3)$, $\mathrm{SU}(2)$ multiplications.

Verifying the code

- **Unit testing.** $\mathrm{SU}(3)$, $\mathrm{SU}(2)$ multiplications.
- **Integration testing.** Random matrix generation, lattice objects, parallelization, ect.

Verifying the code

- **Unit testing.** $\mathrm{SU}(3)$, $\mathrm{SU}(2)$ multiplications.
- **Integration testing.** Random matrix generation, lattice objects, parallelization, ect.
- **Validation testing.** Cross checking results with a configuration from Chroma.

Additional ensembles

Ensemble	N	N_T	N_{cfg}	N_{corr}	N_{up}	a [fm]	L [fm]
E	8	16	8135	600	30	0.0931(4)	0.745(3)
F	12	24	1341	200	20	0.0931(4)	1.118(5)
G	16	32	2000	400	20	0.0790(3)	1.265(6)

- Additional ensembles made in order to illuminate additional aspects of the topological charge.
- Supporting ensembles made on Smaug. All ensembles were flown $N_{\mathrm{flow}} = 1000$ steps with $\epsilon_{\mathrm{flow}} = 0.01$.

Verifying the integration

Testing the integrator for different integration steps ϵ_f.

ϵ_f	0.001	0.005	0.007	0.009	0.01	0.02	0.03	0.05	0.1	0.5

- The values we will test the integrator against.

Lattice size $N^3 \times N_T = 24^3 \times 48$ with $\beta = 6.0$.

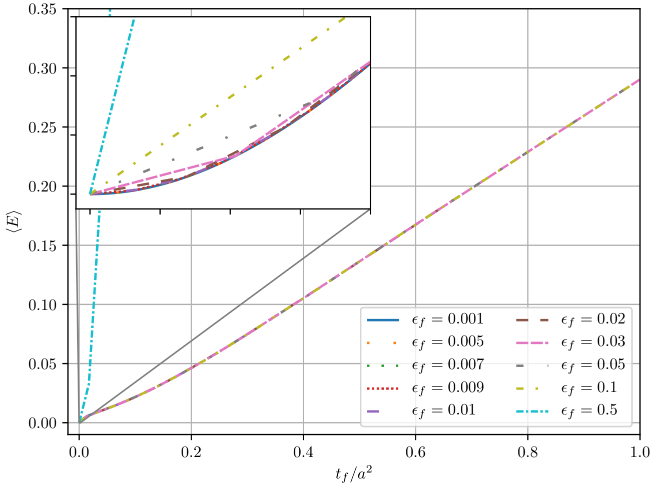

- The values we will test the integrator against.
- The energy flowed for different the different ϵ_f values.

The absolute difference between the smallest flow time $\epsilon_f = 0.001$ and those shown previously.

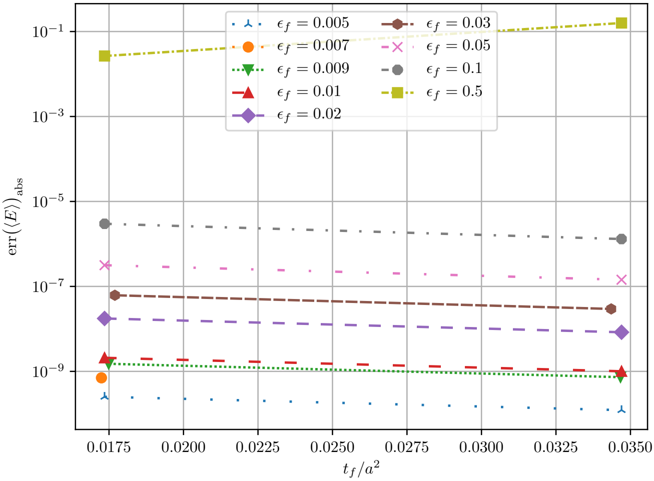

- The values we will test the integrator against.
- The energy flowed for different the different ϵ_f values.
- The absolute difference between the smallest flow time $\epsilon_f = 0.001$ and those listed in previous table.
- The reason for **only having two points** is due to the fact that we are only **comparing points** that are **close to each other in flow time**. If we were to have more points, we would have to double the number of flow time steps for the smallest lattices.

The absolute difference between the smallest flow time $\epsilon_f = 0.001$ and those shown previously.

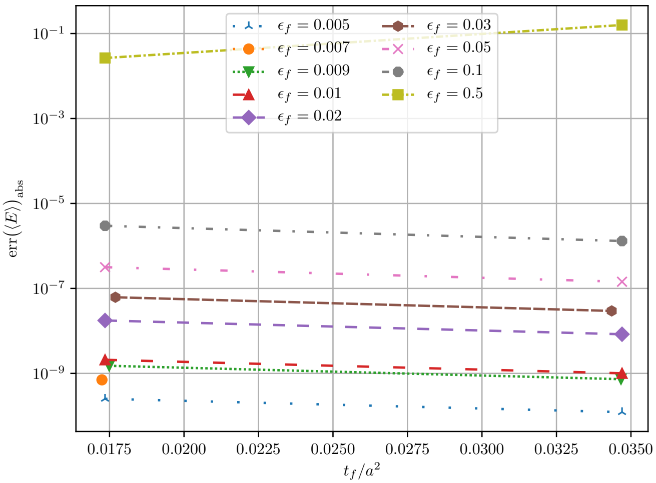

- The values we will test the integrator against.
- The energy flowed for different the different ϵ_f values.
- The absolute difference between the smallest flow time $\epsilon_f = 0.001$ and those listed in previous table.
- The reason for **only having two points** is due to the fact that we are only **comparing points** that are **close to each other in flow time**. If we were to have more points, we would have to double the number of flow time steps for the smallest lattices.
- An **example** of the flowing, can be seen by observing the **energy evolving over flow time**.

The absolute difference between the smallest flow time $\epsilon_f = 0.001$ and those shown previously.

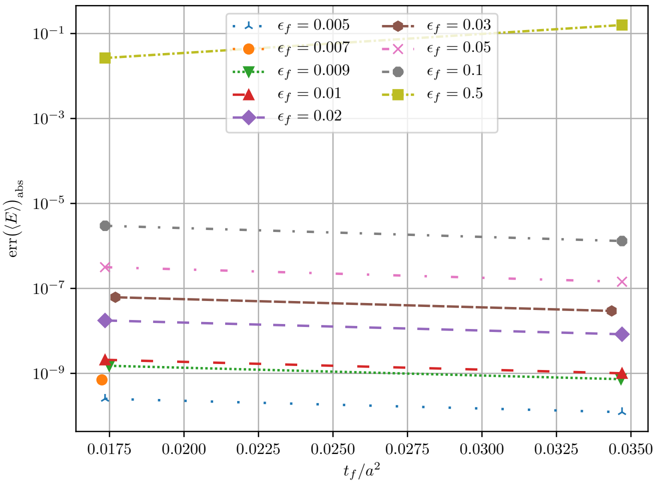

- The values we will test the integrator against.
- The energy flowed for different the different ϵ_f values.
- The absolute difference between the smallest flow time $\epsilon_f = 0.001$ and those listed in previous table.
- The reason for **only having two points** is due to the fact that we are only **comparing points** that are **close to each other in flow time**. If we were to have more points, we would have to double the number of flow time steps for the smallest lattices.
- An **example** of the flowing, can be seen by observing the **energy evolving over flow time**.